

# The Space of Functions Computed By Deep Layered Machines

Alexander Mozeika,<sup>1,\*</sup> Bo Li,<sup>2,†</sup> and David Saad<sup>2,‡</sup>

<sup>1</sup>London Institute for Mathematical Sciences, London, W1K 2XF, United Kingdom

<sup>2</sup>Non-linearity and Complexity Research Group, Aston University, Birmingham, B4 7ET, United Kingdom

We study the space of Boolean functions computed by random layered machines, including deep neural networks, and Boolean circuits. Investigating recurrent and layered feed-forward architectures, we find that the spaces of functions realized by both architectures are the same. We show that, depending on the initial conditions and computing elements used, the entropy of Boolean functions computed by deep layered machines is either monotonically increasing or decreasing with growing depth, and characterize the space of functions computed at the large depth limit.

Deep layered machines comprise multiple consecutive layers of basic computing elements, aimed at representing an arbitrary function, where the first and final layers represent its input and output arguments, respectively. Notable examples include deep neural networks (DNNs) composed of basic perceptrons at each layer [1] and layered Boolean circuits comprising basic logical gates [2]. DNNs are powerful learning machines with large approximability capabilities [3, 4], which have been successfully applied to different machine learning applications [1]. Similarly, layered Boolean circuits can compute arbitrary Boolean functions even when they are constructed from a single elementary gate [5].

While research into DNNs focuses on their application in carrying out specific complex tasks, it is equally important to establish the space of functions they are capable of representing for given architectures, primarily the computing elements used, layer width and depth. Such a generic study requires considering a complete ensemble of DNNs where inter-layer connecting weights are sampled at random. The study of neural networks with random weights using methods of statistical physics has played an important role in understanding their *typical* case properties of storage capacity [6] and generalization ability [7]. In parallel, there have been theoretical studies within the computer science community, of the range of Boolean functions generated by randomly-connected layered Boolean circuits [5, 8]. Both frameworks share common basic properties.

Characterizing the space of functions computed by random layered machines is of great importance, since it impacts on their approximation and generalization abilities. However, it is also highly challenging due to the recursive application of nonlinear functions and inherent randomness of the cross-layer connections, manifested in the weight values and connectivity. Existing analyses of the function space of deep layered machines are mostly based on the mean field behavior, which allows for a sensitivity analysis of the generated functions due to input or parameter perturbations [4, 9–11]. To gain a complete and detailed understanding of the function space, we develop a generating functional formalism that directly examines *individual functions* in function space. This is carried out

by processing *all possible input configurations simultaneously and the corresponding outputs*. For simplicity, we always consider binary input and output variables such that Boolean functions are being implemented. The main contribution of the paper is in providing full understanding of the space of functions, based on the number of different individual functions implemented, pointing to the equivalence between recurrent and layered machines and the dependence of function space on the number of layers and nonlinearity used.

*Framework*—The layered machines considered consist of  $L + 1$  layers, each with  $N$  nodes. Node  $i$  at layer  $l$  is connected to the set of nodes  $\{i_1, i_2, \dots, i_k\}$  of layer  $l - 1$ ; its activity is determined by the gate  $\alpha_i^l$ , computing a function of  $k$  inputs, according to the propagation rule

$$P(S_i^l | \vec{S}^{l-1}) = \delta(S_i^l, \alpha_i^l(S_{i_1}^{l-1}, S_{i_2}^{l-1}, \dots, S_{i_k}^{l-1})), \quad (1)$$

where  $\delta$  is the Dirac or Kronecker delta function, depending on the domain of  $S_i^l$ . The probabilistic form of Eq. (1) adopted here is convenient for the generating functional analysis and inclusion of noise [10, 12]. We primarily consider two structures here: (i) densely connected models where  $k = N$  and node  $i$  is connected to all nodes from the previous layer; one such example is the fully-connected neural network with  $S_i^l = \alpha^l(H_i^l)$ , where  $H_i^l = \sum_{j=1}^N W_j^l S_j^{l-1} / \sqrt{N} + b_i^l$  is the pre-activation field and  $\alpha^l$  is the activation function at layer  $l$ , (we will mainly focus on the case  $b_i^l = 0$ , the effect on non-zero bias is discussed in [13]); (ii) sparsely connected models where  $k \in O(N^0)$ ; examples include the sparse neural networks and layered Boolean circuits where  $\alpha_i^l$  is a Boolean gate with  $k$  inputs, e.g., majority gate.

Consider a binary input vector  $\vec{s} = (s_1, \dots, s_n) \in \{-1, 1\}^n$ , which is fed to the initial layer  $l = 0$ . To accommodate a broader set of functions, we also consider an augmented input vector, e.g., (i)  $\vec{S}^I = (\vec{s}, 1)$ , which is equivalent to adding a bias variable in the context of neural networks; (ii)  $\vec{S}^I = (\vec{s}, -\vec{s}, 1, -1)$ , which has been used to develop unbiased Boolean functions [5]. Each node  $i$  at layer 0 points to a randomly chosen element of

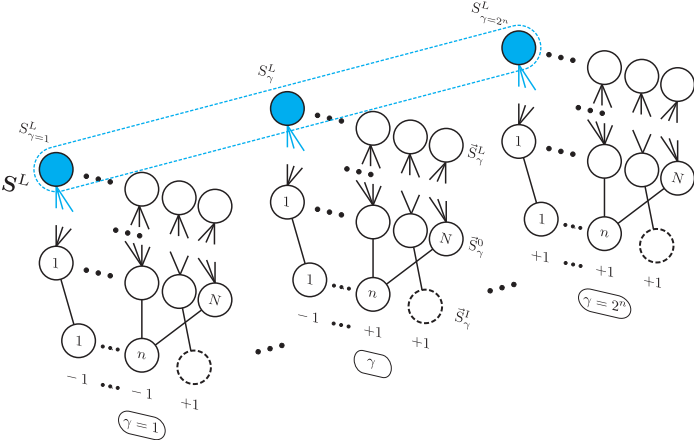


Figure 1. A deep layered machine processing all possible  $2^n$  inputs. The binary string  $\mathbf{S}^L \in \{-1, 1\}^{2^n}$  represents the Boolean function computed on the blue nodes. The augmented input vector  $\vec{S}^I = (\vec{s}, 1)$  is used as an example here. The constant 1 is represented by the dashed circle.

$\vec{S}^I$  such that

$$P^0(\vec{S}^0|\vec{s}) = \prod_{i=1}^N P^0(S_i^0|S_{n_i}^I(\vec{s})) = \prod_{i=1}^N \delta(S_i^0, S_{n_i}^I(\vec{s})), \quad (2)$$

where  $n_i = 1, \dots, |\vec{S}^I|$  is an index chosen from the flat distribution  $P(n_i) = 1/|\vec{S}^I|$ .

The computation of the layered machine is governed by the propagator  $P(\vec{S}^L|\vec{s}) = \sum_{\vec{s}^{L-1} \dots \vec{s}^0} P(\vec{S}^0|\vec{s}) \prod_{l=1}^L P(\vec{S}^l|\vec{S}^{l-1})$ , where each node at layer  $L$  computes a Boolean function  $F : \{-1, 1\}^n \rightarrow \{-1, 1\}$ . When the gates  $\alpha_i^l$  or the layered network topology are *random*, then the layered machine can be viewed as a disordered dynamical system with *quenched* disorder [10, 12]. To probe the functions being computed, we consider the simultaneous layer propagation of *all* possible inputs  $\vec{s}_\gamma \in \{-1, 1\}^n$ , labeled by  $\gamma = 1, \dots, 2^n$  governed by the product propagator  $\rho(\{\vec{S}_\gamma^L\}) = \prod_{\gamma=1}^{2^n} P(\vec{S}_\gamma^L|\vec{s}_\gamma)$ . The binary string  $\mathbf{S}_i^L \in \{-1, 1\}^{2^n}$  represents the Boolean function computed at node  $i$  at layer  $L$ , as illustrated in Fig. 1. Note that we use the vector notation  $\vec{S}^l = (S_1^l, \dots, S_i^l, \dots, S_N^l)$  and  $\mathbf{S}_i^l = (S_{i,1}^l, \dots, S_{i,\gamma}^l, \dots, S_{i,2^n}^l)$  to represent the states and functions, respectively. Using above formalism, the probability of Boolean function  $F$  being computed in the final layer is

$$P(F) = \left\langle \frac{1}{N} \sum_{i=1}^N \prod_{\gamma=1}^{2^n} \delta(S_{i,\gamma}^L, F(s_{1,\gamma}, \dots, s_{n,\gamma})) \right\rangle_\rho. \quad (3)$$

Angled brackets represent an average over entire mappings  $\rho(\{\vec{S}_\gamma^L\})$ . To characterize  $P(F)$  and compute averages of other macroscopic *observables*, which are expected to be self-averaging for  $N \rightarrow \infty$  [14], we introduce

the disorder-averaged generating functional (GF)  $\overline{\Gamma}[\psi] = \overline{\sum_{\{S_{i,\gamma}^l\}} \prod_\gamma P(\vec{S}_\gamma^L|\vec{s}_\gamma^I) \exp(-i \sum_{l,i,\gamma} \psi_{i,\gamma}^l S_{i,\gamma}^l)}$ , where overline denotes an average over quenched variables. To keep the presentation concise, we outline the GF formalism only for DNNs in the following and refer the reader to [13] for the details of the derivation used in Boolean circuits.

*Layered and recurrent architectures*—We focus on two different architectures: layered, where the gates and/or connections are different from layer to layer, and recurrent architectures, where the gates and connections are shared across all layers, which are analogous to time steps. Both architectures represent feed-forward machines that implement input-output mappings.

Specifically, the weights  $W_{ij}^l$  of fully-connected DNNs with layered architectures are the layer-dependent Gaussian random variables with  $W_{ij}^l \sim \mathcal{N}(0, \sigma_w^2)$ . In DNNs with recurrent architectures, the weights are sampled once and are shared among layers, i.e.  $W_{ij}^l = W_{ij}$ . We apply sign activation function in the final layer of DNNs, i.e.  $\alpha^L(H_i^L) = \text{sgn}(H_i^L)$ , to ensure that the outputs  $S_i^L$  are Boolean.

We first outline the derivation for densely-connected recurrent architectures. It is sufficient to characterize the disorder-averaged GF by introducing cross-layer overlaps  $q_{\gamma\gamma'}^{l,l'} = (1/N) \langle \sum_i S_{i,\gamma}^l S_{i,\gamma'}^{l'} \rangle_\rho$  as order parameters and the corresponding conjugate order parameter  $Q_{\gamma\gamma'}^{l,l'}$ , which leads to a saddle-point integral  $\overline{\Gamma} = \int \{d\mathbf{q}d\mathbf{Q}\} e^{N\Psi[\mathbf{q},\mathbf{Q}]}$  with the potential [13]

$$\Psi = i \sum_{l,l',\gamma,\gamma'} Q_{\gamma\gamma'}^{l,l'} q_{\gamma\gamma'}^{l,l'} + \sum_{m=1}^{|\vec{S}^I|} P(m) \ln \int_{\{S_i^l\}} d\mathbf{H} \sum_{\{\mathbf{S}\}} \mathcal{M}_m(\mathbf{H}, \mathbf{S}) \quad (4)$$

where  $\mathcal{M}_m(\mathbf{H}, \mathbf{S})$  is an effective single-site measure

$$\mathcal{M}_m = e^{-i \sum_{l,\gamma} \psi_\gamma^l S_\gamma^{l-1} - i \sum_{l,l',\gamma,\gamma'} Q_{\gamma\gamma'}^{l,l'} S_\gamma^l S_{\gamma'}^{l'}} \prod_{\gamma=1}^{2^n} P^0(S_\gamma^0|S_{m,\gamma}^I) \times \mathcal{N}(\mathbf{H}|\mathbf{0}, \mathbf{C}(\mathbf{q})) \prod_{l=1}^L \prod_{\gamma=1}^{2^n} \delta(S_\gamma^l, \alpha^l(H_\gamma^l)). \quad (5)$$

representing the joint mean field distribution of the layered dynamics. Due to weight-sharing, the  $2^n L$  dimensional pre-activation fields  $\mathbf{H}$ , governed by the Gaussian distribution  $\mathcal{N}(\mathbf{H}|\mathbf{0}, \mathbf{C}(\mathbf{q}))$  in Eq. (5), are correlated across layers with covariance  $\mathbf{C}_{\gamma\gamma'}^{l,l'} = \sigma_w^2 q_{\gamma\gamma'}^{l-1,l'-1}$ . Setting  $\psi_\gamma^l$  to zero and differentiating  $\Psi$  with respect to  $\{q_{\gamma\gamma'}^{l,l'}, Q_{\gamma\gamma'}^{l,l'}\}$  yields the saddle point of the potential  $\Psi$  dominating  $\overline{\Gamma}$ , at which the conjugate order parameters vanish [13], leading to

$$q_{\gamma\gamma'}^{l,l'} = \begin{cases} \sum_m P(m) \langle S_\gamma^l S_{\gamma'}^0 \rangle_{\mathcal{M}_m}, & l' = 0 \\ \int d\mathbf{H} \alpha^l(H_\gamma^l) \alpha^{l'}(H_{\gamma'}^{l'}) \mathcal{N}(\mathbf{H}|\mathbf{0}, \mathbf{C}(\mathbf{q})). & l' > 0 \end{cases} \quad (6)$$

Notice that in the Gaussian integral in Eq. (6), all pre-activation fields, but the pair  $\{H_\gamma^l, H_{\gamma'}^{l'}\}$ , can be integrated out, reducing it to a tractable two-dimensional integral.

The GF analysis can be performed similarly on layered architectures, which share the same structure with recurrent ones. For layered architectures, cross-layer overlaps are absent while same-layer order parameters coincide with those of recurrent architectures, i.e.  $q_{\gamma\gamma'}^{l,l'} = \delta_{l,l'} q_{\gamma\gamma'}^{l,l}$  [13]. It implies that  $\mathcal{C}_{\gamma\gamma'}^{l,l'} = \sigma_w^2 \delta_{l-1,l'-1} q_{\gamma\gamma'}^{l-1,l'-1}$  for the covariances of pre-activation fields.

We remark that the behavior of the DNNs with layered architectures can also be obtained by mapping the DNNs to Gaussian processes in the limit  $N \rightarrow \infty$  using the central limit theorem [4, 9, 15]; however, it is not clear if such analysis is possible in the highly correlated recurrent architectures while the GF is easily applicable [16].

By marginalizing the single-site measure  $\mathcal{M}$  in Eq. (5), one obtains the joint distribution of pre-activation fields  $\mathbf{H}^L$  and activities  $\mathbf{S}^L$  at layer  $L$  in the recurrent architectures as

$$P(\mathbf{H}^L, \mathbf{S}^L) = \mathcal{N}(\mathbf{H}^L | \mathbf{0}, \mathcal{C}^{L,L}) \prod_{\gamma=1}^{2^n} \delta(S_\gamma^L, \alpha^L(H_\gamma^L)), \quad (7)$$

where the covariance is given by  $\mathcal{C}_{\gamma\gamma'}^{L,L} = \sigma_w^2 q_{\gamma\gamma'}^{L-1,L-1}$ . Notably, Eq. (7) also applies to layered architectures since the *same-layer* covariances  $\mathcal{C}^{L,L}$  in the two scenarios are identical. Therefore we arrive at the first important conclusion that *the typical sets of functions computed at the output layer  $L$  by the layered and recurrent architectures are identical*. Furthermore, if the gate functions  $\alpha^l$  are odd, then it can be shown that all the cross-layer overlaps  $q_{\gamma\gamma'}^{l,l'}$  of the recurrent architectures vanish, implying the statistical equivalence of the hidden layer activities to the layered architectures as well [13].

We can apply a similar analysis to sparsely-connected Boolean circuits constructed from a single-form Boolean gate  $\alpha$ , keeping in mind that distributions of gates can be easily accommodated. In such models, the disorder comes from random connections rather than random gates. In layered architectures, a gate is connected randomly to exactly  $k \in O(N^0)$  gates from the previous layer and this connectivity pattern is changing from layer to layer. In recurrent architectures, on the other hand, the random connections are sampled once and the connectivity pattern is shared among layers. For layered architectures, the GF analysis gives rise to the propagation rule of the probability of the Boolean function

$$\mathbf{S}^l \in \{-1, 1\}^{2^n} \quad [13]$$

$$P^{l+1}(\mathbf{S}^{l+1}) = \sum_{\{\mathbf{S}_j^l\}_{\forall j}} \left\{ \prod_{j=1}^k P^l(\mathbf{S}_j^l) \right\} \times \prod_{\gamma=1}^{2^n} \delta(S_\gamma^{l+1}, \alpha(S_{1,\gamma}^l, \dots, S_{k,\gamma}^l)). \quad (8)$$

While for recurrent architectures the activities at different layers  $\{\mathbf{S}^l\}_{\forall l}$  are correlated due to the recurrent topology. Interestingly, if only the single-layer activities are of interest, the layer propagation rule has the same expression as Eq. (8) [13]. It suggests that *the function spaces computed by the output layer of the random machines of both architectures are also identical*.

*The space of computed Boolean functions*—We then characterize the functions being computed by the random layered machines by examining  $P(\mathbf{S}^L)$  in the large depth limit, which depend on the non-linear activation functions or Boolean gates used as illustrated in the following examples.

For DNNs using the popular ReLU activation function  $\alpha^l(x) = \max(x, 0)$  in the hidden layers (sign activation function is always used in the output layer), all the matrix elements  $\{\mathcal{C}_{\gamma\gamma'}^{L,L}\}$  converge to the same value in the limit  $L \rightarrow \infty$ . It implies that all pre-activation fields  $\{H_\gamma^L\}_{\forall \gamma}$  converge to the same value, such that all the outputs  $\{S_\gamma^L\}_{\forall \gamma}$  are identical. This is due to the fact the ReLU activation function keeps only the positive part of the pre-activation field, which introduces correlation among patterns. Therefore, deep ReLU networks compute only *constant* functions in the infinite depth limit [17], echoing recent findings of simplicity bias in random ReLU DNNs [11, 18, 19].

For DNNs using sign activation functions and in the *absence* of bias variables, the cross-pattern overlaps satisfying  $|q_{\gamma\gamma'}^l| < 1$  monotonically decrease with increasing  $l$  and converge to zero in the large  $L$  limit; the chaotic nature of the dynamics also holds in random DNNs with other sigmoidal activation functions such as the error function and hyperbolic tangent [4, 15], which share similar properties to those of DNNs with sign activation functions. To examine how general this behavior is, we compute  $P(F) = \int d\mathbf{H}^L \sum_{\mathbf{S}^L} P(\mathbf{H}^L, \mathbf{S}^L) \prod_\gamma \delta(S_\gamma^L, F(\vec{s}_\gamma))$ ; it is easy to show that for input vector  $\vec{S}^I = \vec{s}$ , DNNs compute *all odd functions* (satisfying  $F(-\vec{s}_\gamma) = -F(\vec{s}_\gamma)$ ) *with equal probability* [15]; the restriction to odd functions is due to the parity symmetry of the perceptron  $S_i^l = \text{sgn}(\sum_j W_{ij}^l S_j^{l-1} / \sqrt{N})$  and the initial condition. Moreover, for  $\vec{S}^I = (\vec{s}, 1)$ , the additional constant variable breaks the symmetry in the initial layer, and eventually leads to a *uniform distribution of all Boolean functions* being computed  $P(F) = 1/2^{2^n}$ . While in the presence of random bias variables, the cross-pattern overlaps converge to a nonzero constant and the variability of the

functions being computed is lower [13].

For layered Boolean circuits in the large  $L$  limit, it is also known that the generated functions either converge to a single Boolean function or to the uniform distribution over functions [5, 8, 20], depending on the gates used and the mapping between the input and layer 0. For example, for AND gates with  $\alpha(S_1, S_2) = \text{sgn}(S_1 + S_2 + 1)$  and OR gate with  $\alpha(S_1, S_2) = \text{sgn}(S_1 + S_2 - 1)$  [13], the single gate outputs are biased towards  $+1$  and  $-1$ , respectively. By analyzing the marginal probability  $P(S_\gamma^l)$ , it can be shown that *the corresponding layered Boolean circuits eventually converge to a single Boolean function in deep layers* [13, 20].

On the other hand, the majority vote gate  $\alpha(S_1, \dots, S_k) = \text{sgn}(\sum_{j=1}^k S_j)$ , where  $k$  is odd, is balanced, i.e.  $\sum_{S_1, \dots, S_k} \alpha(S_1, \dots, S_k) = 0$  and non-linear [21]. If a balanced input  $\vec{S}^I = (\vec{s}, -\vec{s}, 1, -1)$  is applied, the corresponding layered machines converge to a *uniform distribution on all Boolean functions* [5, 13, 20].

*Entropy of functions*—Having mentioned a few examples where layered machines either converge to a single function or compute all functions with a uniform probability in the infinite  $L$  limit, we will now examine their properties systematically for finite  $L$  and monitor the evolution of corresponding function distribution. We consider the Shannon entropy at layer  $l$ ,  $\mathcal{H}^l = -\sum_{\mathbf{S}^l} P^l(\mathbf{S}^l) \log P^l(\mathbf{S}^l)$ , where  $\mathcal{H}^L$  is equivalent to the entropy of generated functions  $\mathcal{H}[F] = -\sum_F P(F) \log P(F)$ , which can be calculated from the Eqs. (7) and (8). In Fig. 2, we demonstrate the entropy  $\mathcal{H}^L$  as a function of depth  $L$  for layered machines processing finite inputs using different gate functions. The increase in entropy after layer  $L = 0$  suggests that in these cases, new functions are being created by applying nonlinear gates to the initial layer  $\vec{S}^0$  that is constrained by the input  $\vec{S}^I$ . Note that the minimal depth  $L$  of ReLU networks to produce Boolean output is 2. The behaviors of entropies  $\mathcal{H}^L$  after the initial increase depend on the specific gate functions used. For biased gate functions, e.g., ReLU activation in DNNs and AND gate in Boolean circuits, the entropies  $\mathcal{H}^L$  monotonically decrease with  $L$ , suggesting that a smaller set of functions is computed in the corresponding machines with deeper layers. Initializing layered machines with such gate functions by using random weights or random connections, places a biasing prior towards a restricted set of functions [18, 19]. On the other hand, for balanced gate functions with appropriate initial conditions, e.g., sign activation in DNNs and majority vote gate in Boolean circuits, the entropies  $\mathcal{H}^L$  monotonically increase with  $L$ , which indicates that a broader set of functions is computed in layered machines with deeper layers.

In summary, we presented an analytical framework to examine Boolean functions computed by random deep layered machines, by considering all possible inputs si-

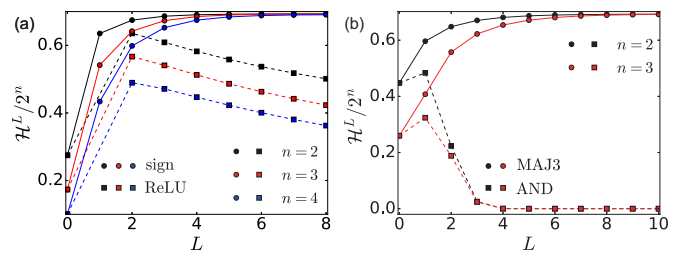


Figure 2. Entropy of Boolean functions  $\mathcal{H}^L$ , normalized by  $2^n$ , as a function of the network depth  $L$ . (a) DNNs with sign or ReLU activation functions in the hidden layers; the initial condition is set as  $\vec{S}^I = (\vec{s}, 1)$ . (b) Layered Boolean circuits constructed by MAJ-3 gate or AND gate with initial condition  $\vec{S}^I = (\vec{s}, -\vec{s}, 1, -1)$ .

multaneously and applying the generating functional analysis to compute various relevant macroscopic quantities. We derived the probability of functions computed on the output nodes. Surprisingly, we discovered that the spaces of Boolean functions computed by the layered architectures and recurrent architectures are identical. It points to the possibility of computing complex functions with a reduced number of parameters by weight or connection sharing; although whether it is easy or not to identify the suitable weight parameters or connections for specific tasks (i.e., trainability) remains to be explored. We then characterized the space of functions being computed by some specific layer machines. Biased activation functions (e.g., ReLU) or Boolean gates (e.g., AND/OR) can lead to a restricted set of Boolean functions being computed typically at deeper layers. On the other hand, balanced activation functions (e.g., sign) or Boolean gates (e.g., majority gate) complemented with appropriate initial conditions, can lead to a uniform distribution on all functions in the infinite depth limit. We also showed the monotonic changes in the entropy of functions as the Boolean circuits become deeper, which is of interest in the field of computer science. We envisage that the insights gained and the methods developed in this study could facilitate studying other interesting and relevant properties of deep layered machines.

BL and DS acknowledge support from the Leverhulme Trust (RPG-2018-092), European Union’s Horizon 2020 research and innovation programme under the Marie Skłodowska-Curie grant agreement No. 835913. DS acknowledges support from the EPSRC programme grant TRANSNET (EP/R035342/1).

\* alexander.mozeika@kcl.ac.uk

† b.li10@aston.ac.uk

‡ d.saad@aston.ac.uk

[1] Yann LeCun, Yoshua Bengio, and Geoffrey Hinton. Deep learning. *Nature*, 521(7553):436–444, May 2015.



- [2] Ryan O'Donnell. *Analysis of Boolean Functions*. Cambridge University Press, New York, 2014.
- [3] Kurt Hornik, Maxwell Stinchcombe, and Halbert White. Multilayer feedforward networks are universal approximators. *Neural Networks*, 2(5):359 – 366, 1989.
- [4] Ben Poole, Subhaneil Lahiri, Maithreyi Raghunathan, Jascha Sohl-Dickstein, and Surya Ganguli. Exponential expressivity in deep neural networks through transient chaos. In D. D. Lee, M. Sugiyama, U. V. Luxburg, I. Guyon, and R. Garnett, editors, *Advances in Neural Information Processing Systems 29*, pages 3360–3368. Curran Associates, Inc., New York, 2016.
- [5] Petr Savický. Random boolean formulas representing any boolean function with asymptotically equal probability. *Discrete Mathematics*, 83(1):95 – 103, 1990.
- [6] Andreas Engel and Christian Van den Broeck. *Statistical Mechanics of Learning*. Cambridge University Press, New York, 2001.
- [7] David Saad, editor. *On-Line Learning in Neural Networks*. Cambridge University Press, New York, 1998.
- [8] Alex Brodsky and Nicholas Pippenger. The boolean functions computed by random boolean formulas or how to grow the right function. *Random Structures & Algorithms*, 27(4):490–519, 2005.
- [9] Jaehoon Lee, Jascha Sohl-dickstein, Jeffrey Pennington, Roman Novak, Sam Schoenholz, and Yasaman Bahri. Deep neural networks as gaussian processes. In *Proceedings of the 6th International Conference on Learning Representations, 2018*.
- [10] Bo Li and David Saad. Exploring the function space of deep-learning machines. *Phys. Rev. Lett.*, 120:248301, Jun 2018.
- [11] Bo Li and David Saad. Large deviation analysis of function sensitivity in random deep neural networks. *Journal of Physics A: Mathematical and Theoretical*, 53(10):104002, feb 2020.
- [12] Alexander Mozeika, David Saad, and Jack Raymond. Computing with noise: Phase transitions in boolean formulas. *Phys. Rev. Lett.*, 103:248701, 2009.
- [13] See Supplemental Material for details, which includes Ref. [22].
- [14] Marc Mézard, Giorgio Parisi, and Miguel Virasoro. *Spin glass theory and beyond: An Introduction to the Replica Method and Its Applications*, volume 9. World Scientific Publishing Co Inc, 1987.
- [15] Greg Yang and Hadi Salman. A fine-grained spectral perspective on neural networks. arXiv:1907.10599, 2019.
- [16] A.C.C. Coolen. Chapter 15 statistical mechanics of recurrent neural networks ii - dynamics. In F. Moss and S. Gielen, editors, *Neuro-Informatics and Neural Modelling*, volume 4 of *Handbook of Biological Physics*, pages 619 – 684. North-Holland, 2001.
- [17] Arnu Pretorius, Elan van Biljon, Steve Kroon, and Herman Kamper. Critical initialisation for deep signal propagation in noisy rectifier neural networks. In S. Bengio, H. Wallach, H. Larochelle, K. Grauman, N. Cesa-Bianchi, and R. Garnett, editors, *Advances in Neural Information Processing Systems 31*, pages 5717–5726. Curran Associates, Inc., 2018.
- [18] Guillermo Valle-Perez, Chico Q. Camargo, and Ard A. Louis. Deep learning generalizes because the parameter-function map is biased towards simple functions. In *Proceedings of the 7th International Conference on Learning Representations*. 2019.
- [19] Giacomo De Palma, Bobak Kiani, and Seth Lloyd. Random deep neural networks are biased towards simple functions. In H. Wallach, H. Larochelle, A. Beygelzimer, F. d'Alché-Buc, E. Fox, and R. Garnett, editors, *Advances in Neural Information Processing Systems 32*, pages 1962–1974. Curran Associates, Inc., 2019.
- [20] Alexander Mozeika, David Saad, and Jack Raymond. Noisy random boolean formulae: A statistical physics perspective. *Phys. Rev. E*, 82:041112, 2010.
- [21] Since  $\{S_j\}$  are binary variables in the context of Boolean circuits, linearity is defined in the finite field  $GF(2)$  [5, 8].
- [22] Taro Toyozumi and Haiping Huang. Structure of attractors in randomly connected networks. *Phys. Rev. E*, 91:032802, Mar 2015.

# The Functions Computed by Deep Layered Machines Supplemental Material

Alexander Mozeika,<sup>1</sup> Bo Li,<sup>2</sup> and David Saad<sup>2</sup>

<sup>1</sup>*London Institute for Mathematical Sciences, London, W1K 2XF, United Kingdom*

<sup>2</sup>*Non-linearity and Complexity Research Group, Aston University, Birmingham, B4 7ET, United Kingdom*

## I. CONVENTION OF NOTATION

We denote variables with overarrows as vectors with site indices (e.g.,  $i, j$ ), which can be of size  $k, n$  or  $N$ . On the other hand, we denote bold-symbol variables as vectors with pattern indices (e.g.,  $\gamma, \gamma'$ ), which are of size  $2^n$ . For convenience, we define  $M := 2^n$ .

The function  $\delta(\cdot, \cdot)$  stands for Kronecker delta as  $\delta(i, j) = \delta_{i,j}$  if arguments  $i, j$  are integer variables, while it stands for Dirac delta function as  $\delta(x, y) = \delta(x - y)$  if the arguments  $x, y$  are continuous variables; in the latter case, the summation operation should be interpreted as integration, such that  $\sum_y \delta(x, y)f(y) := \int dy \delta(x - y)f(y)$ .

The binary variables  $S \in \{+1, -1\}$  in this work are mapped onto the conventional Boolean variables  $z \in \{0, 1\}$  through  $S = 1 - 2z$ .

## II. GENERATING FUNCTIONAL ANALYSIS OF FULLY-CONNECTED NEURAL NETWORKS

To probe the functions being computed by neural networks, we need to consider the layer propagation of all  $2^n$  input patterns as  $\prod_{\gamma=1}^{2^n} P(\vec{S}_\gamma^L | \vec{S}_\gamma^I(\vec{s}_\gamma))$ . We introduce the disorder-averaged generating functional in order to compute the macroscopic quantities

$$\begin{aligned} \overline{\Gamma[\{\psi_{i,\gamma}^l\}]} &= \overline{\sum_{\{S_{i,\gamma}^l\}_{\forall l,i,\gamma}} \prod_{\gamma=1}^{2^n} P(\vec{S}_\gamma^0 | \vec{S}_\gamma^I) \prod_{l=1}^L P(\vec{S}_\gamma^l | \vec{S}_\gamma^{l-1}) e^{-i \sum_{l,i,\gamma} \psi_{i,\gamma}^l S_{i,\gamma}^l}} \\ &= \mathbb{E}_W \sum_{\{S_{i,\gamma}^l\}_{\forall l,i,\gamma}} \int \prod_{l=1}^L \prod_{i,\gamma} \frac{dH_{i,\gamma}^l dx_{i,\gamma}^l}{2\pi} \prod_{\gamma=1}^{2^n} P(\vec{S}_\gamma^0 | \vec{S}_\gamma^I) \prod_{l=1}^L P(\vec{S}_\gamma^l | \vec{H}_\gamma^l) e^{-i \sum_{l,i,\gamma} \psi_{i,\gamma}^l S_{i,\gamma}^l} \\ &\quad \times \exp \left[ \sum_{l,i,\gamma} i x_{i,\gamma}^l H_{i,\gamma}^l - \sum_{l,\gamma} \sum_{ij} \frac{i}{\sqrt{N}} W_{ij}^l x_{i,\gamma}^l S_{j,\gamma}^{l-1} \right], \end{aligned} \quad (S1)$$

where we have introduced the notation  $P(\vec{S}_\gamma^l | \vec{H}_\gamma^l) = \prod_{i=1}^N P(S_{i,\gamma}^l | H_{i,\gamma}^l) = \prod_{i=1}^N \delta(S_{i,\gamma}^l, \alpha^l(H_{i,\gamma}^l))$  and inserted the Fourier representation of unity  $1 = \int \frac{dH_{i,\gamma}^l dx_{i,\gamma}^l}{2\pi} \exp [i x_{i,\gamma}^l (H_{i,\gamma}^l - \sum_j W_{ij}^l S_{j,\gamma}^{l-1})]$ ,  $\forall l, i, \gamma$ . Noisy computation can be easily accommodated in such probabilistic formalism.

### A. Layered Architectures

We first consider layer-dependent weights, where each element follows the Gaussian distribution  $W_{ij}^l \sim \mathcal{N}(0, \sigma_w^2)$ . Assuming self-averaging, averaging over the weight disorder component in the last line of the Eq. (S1) yields

$$\begin{aligned} &\mathbb{E}_W \exp \left[ - \sum_{l=1}^L \sum_{\gamma} \sum_{ij} \frac{i}{\sqrt{N}} W_{ij}^l x_{i,\gamma}^l S_{j,\gamma}^{l-1} \right] \\ &= \exp \left[ - \frac{\sigma_w^2}{2} \sum_{l=1}^L \sum_{\gamma, \gamma'} \sum_i x_{i,\gamma}^l x_{i,\gamma'}^l \left( \frac{1}{N} \sum_j S_{j,\gamma}^{l-1} S_{j,\gamma'}^{l-1} \right) \right]. \end{aligned} \quad (S2)$$

By introducing the overlap order parameters  $\{q_{\gamma\gamma'}^l\}_{l=0}^L$  through the Fourier representation of unity

$$1 = \int \frac{dQ_{\gamma\gamma'}^l dq_{\gamma\gamma'}^l}{2\pi/N} \exp \left[ i N Q_{\gamma\gamma'}^l \left( q_{\gamma\gamma'}^l - \frac{1}{N} \sum_j S_{j,\gamma}^l S_{j,\gamma'}^l \right) \right], \quad (S3)$$

the generating functional can be factorized over sites as follows

$$\begin{aligned}
\overline{\Gamma[\{\psi_{i,\gamma}^l\}]} &= \int \prod_{l=0}^L \prod_{\gamma\gamma'} \frac{dQ_{\gamma\gamma'}^l dq_{\gamma\gamma'}^l}{2\pi/N} \exp \left[ iN \sum_{l,\gamma\gamma'} Q_{\gamma\gamma'}^l q_{\gamma\gamma'}^l \right] \\
&\times \exp \left[ \sum_{i=1}^N \log \int \prod_{l=1}^L \prod_{\gamma} dH_{i,\gamma}^l \sum_{\{S_{i,\gamma}^l\}_{\forall l,\gamma}} \mathcal{M}_{n_i}(\mathbf{H}_i, \mathbf{S}_i) \right] \\
&= \int \prod_{l=0}^L \prod_{\gamma\gamma'} \frac{dQ_{\gamma\gamma'}^l dq_{\gamma\gamma'}^l}{2\pi/N} \exp \left[ iN \sum_{l,\gamma\gamma'} Q_{\gamma\gamma'}^l q_{\gamma\gamma'}^l \right] \\
&\times \exp \left[ N \left( \sum_{m=1}^{|\vec{S}^I|} \frac{1}{N} \sum_{i=1}^N \delta(m, n_i) \right) \log \int \prod_{l=1}^L \prod_{\gamma} dH_{i,\gamma}^l \sum_{\{S_{i,\gamma}^l\}_{\forall l,\gamma}} \mathcal{M}_m(\mathbf{H}_i, \mathbf{S}_i) \right],
\end{aligned}$$

where  $\mathbf{H}_i, \mathbf{S}_i$  are shorthand notations of  $\{\mathbf{H}_i^l\}, \{\mathbf{S}_i^l\}$  with  $\mathbf{H}_i^l := (H_{i,1}^l, \dots, H_{i,\gamma}^l, \dots, H_{i,2^n}^l)$  and  $\mathbf{S}_i^l := (S_{i,1}^l, \dots, S_{i,\gamma}^l, \dots, S_{i,2^n}^l)$ . The single-site measure  $\mathcal{M}_m$  in the above expression is defined as

$$\begin{aligned}
\mathcal{M}_m(\mathbf{H}_i, \mathbf{S}_i) &= \prod_{\gamma=1}^{2^n} e^{-i \sum_{l,\gamma} \psi_{i,\gamma}^l S_{i,\gamma}^l} P(S_{i,\gamma}^0 | S_{m,\gamma}^I) \prod_{l=1}^L P(S_{i,\gamma}^l | H_{i,\gamma}^l) \exp \left[ - \sum_{l,\gamma\gamma'} i Q_{\gamma\gamma'}^l S_{i,\gamma}^l S_{i,\gamma'}^l \right] \\
&\times \prod_{l=1}^L \frac{1}{\sqrt{(2\pi)^{2^n} |\mathbf{C}^l|}} \exp \left[ - \frac{1}{2} \sum_{\gamma\gamma'} H_{i,\gamma}^l (\mathbf{C}^l)_{\gamma\gamma'}^{-1} H_{i,\gamma'}^l \right].
\end{aligned} \tag{S4}$$

In Eq. (S4),  $\mathbf{C}^l$  is a  $2^n \times 2^n$  covariance matrix with elements  $\mathbf{C}_{\gamma\gamma'}^l = \sigma_w^2 q_{\gamma\gamma'}^{l-1}$  and  $m$  is a random index following the empirical distribution  $\frac{1}{N} \sum_{i=1}^N \delta(m, n_i)$ .

Setting  $\psi_{i,\gamma}^l = 0$  and considering  $\lim_{N \rightarrow \infty} \frac{1}{N} \sum_{i=1}^N \delta(m, n_i) \rightarrow P(m) = 1/|\vec{S}^I|$ , we arrive at

$$\bar{\Gamma} = \int \{d\mathbf{Q}d\mathbf{q}\} e^{N\Psi(\mathbf{Q},\mathbf{q})}, \tag{S5}$$

$$\Psi(\mathbf{Q}, \mathbf{q}) = \sum_{l=0}^L \sum_{\gamma\gamma'} i Q_{\gamma\gamma'}^l q_{\gamma\gamma'}^l + \sum_{n=1}^{|\vec{S}^I|} P(n) \log \int \prod_{l=1}^L \prod_{\gamma} dH_{i,\gamma}^l \sum_{\{S_{i,\gamma}^l\}_{\forall l,\gamma}} \mathcal{M}_m(\mathbf{H}, \mathbf{S}). \tag{S6}$$

The saddle point equations are obtained by computing  $\partial\Psi/\partial q_{\gamma\gamma'}^l = 0$  and  $\partial\Psi/\partial Q_{\gamma\gamma'}^l = 0$

$$iQ_{\gamma\gamma'}^{l-1} = - \sum_n P(n) \frac{\int d\mathbf{H} \sum_{\mathbf{S}} \frac{\partial}{\partial q_{\gamma\gamma'}^{l-1}} \mathcal{M}_m(\mathbf{H}, \mathbf{S})}{\int d\mathbf{H} \sum_{\mathbf{S}} \mathcal{M}_m(\mathbf{H}, \mathbf{S})}, \quad 1 \leq l \leq L, \tag{S7}$$

$$iQ_{\gamma\gamma'}^L = 0, \tag{S8}$$

$$q_{\gamma\gamma'}^l = \sum_{m=1}^{|\vec{S}^I|} P(m) \langle S_{i,\gamma}^l S_{i,\gamma'}^l \rangle_{\mathcal{M}_m}, \quad 0 \leq l \leq L. \tag{S9}$$

Back-propagating the boundary condition  $iQ_{\gamma\gamma'}^L = 0$  results in  $iQ_{\gamma\gamma'}^l = 0, \forall l [1]$ .

The measure  $\mathcal{M}_m$  becomes

$$\begin{aligned}
\mathcal{M}_m(\mathbf{H}, \mathbf{S}) &= \prod_{\gamma=1}^{2^n} P(S_{i,\gamma}^0 | S_{m,\gamma}^I) \prod_{l=1}^L P(S_{i,\gamma}^l | H_{i,\gamma}^l) \\
&\times \prod_{l=1}^L \frac{1}{\sqrt{(2\pi)^{2^n} |\mathbf{C}^l|}} \exp \left[ - \frac{1}{2} \sum_{\gamma\gamma'} H_{i,\gamma}^l (\mathbf{C}^l)_{\gamma\gamma'}^{-1} H_{i,\gamma'}^l \right],
\end{aligned} \tag{S10}$$

while the saddle point equations of overlaps have the form of

$$q_{\gamma\gamma'}^0 = \sum_m P(m) S_{m,\gamma}^I S_{m,\gamma'}^I, \quad (\text{S11})$$

$$q_{\gamma\gamma'}^l = \int dH_\gamma^l dH_{\gamma'}^l \frac{\phi^l(H_\gamma^l) \phi^l(H_{\gamma'}^l)}{\sqrt{(2\pi)^2 |\Sigma_{\gamma\gamma'}^l|}} \exp \left[ -\frac{1}{2} [H_\gamma^l, H_{\gamma'}^l] \cdot (\Sigma_{\gamma\gamma'}^l)^{-1} \cdot [H_\gamma^l, H_{\gamma'}^l]^\top \right], \quad (\text{S12})$$

where the  $2 \times 2$  covariance matrix  $\Sigma_{\gamma\gamma'}^l$  is defined as

$$\Sigma_{\gamma\gamma'}^l := \sigma_w^2 \begin{pmatrix} q_{\gamma\gamma}^{l-1} & q_{\gamma\gamma'}^{l-1} \\ q_{\gamma'\gamma}^{l-1} & q_{\gamma'\gamma'}^{l-1} \end{pmatrix}. \quad (\text{S13})$$

## B. Recurrent Architectures

In this section, we consider recurrent topology where the weights are independent of layers  $W_{ij}^l = W_{ij} \sim \mathcal{N}(0, \sigma_w^2)$ . The calculation resembles the case of layer-dependent weights, except that the disorder average yields cross-layer overlaps

$$\begin{aligned} & \mathbb{E}_W \exp \left[ -\sum_{l=1}^L \sum_{\gamma} \sum_{ij} \frac{i}{\sqrt{N}} W_{ij} x_{i,\gamma}^l S_{j,\gamma}^{l-1} \right] \\ &= \exp \left[ -\frac{\sigma_w^2}{2} \sum_{l,l'=1}^L \sum_{\gamma,\gamma'} \sum_i x_{i,\gamma}^l x_{i,\gamma'}^{l'} \left( \frac{1}{N} \sum_j S_{j,\gamma}^{l-1} S_{j,\gamma'}^{l'-1} \right) \right]. \end{aligned} \quad (\text{S14})$$

Introducing order parameters  $q_{\gamma\gamma'}^{l,l'} := \frac{1}{N} \sum_j S_{j,\gamma}^l S_{j,\gamma'}^{l'}$  and setting  $\psi_{i,\gamma}^l = 0$ , we eventually obtain

$$\bar{\Gamma} = \int \{d\mathbf{Q}d\mathbf{q}\} e^{N\Psi(\mathbf{Q},\mathbf{q})}, \quad (\text{S15})$$

$$\Psi(\mathbf{Q}, \mathbf{q}) = \sum_{l,l'=0}^L \sum_{\gamma\gamma'} iQ_{\gamma\gamma'}^{l,l'} q_{\gamma\gamma'}^{l,l'} + \sum_{m=1}^{|\bar{S}^l|} P(m) \log \int \prod_{l=1}^L \prod_{\gamma} dH_\gamma^l \sum_{\{S_\gamma^l\}_{\forall l,\gamma}} \mathcal{M}_m(\mathbf{H}, \mathbf{S}), \quad (\text{S16})$$

$$\begin{aligned} \mathcal{M}_m(\mathbf{H}, \mathbf{S}) &= \prod_{\gamma=1}^{2^n} P(S_\gamma^0 | S_{m,\gamma}^I) \prod_{l=1}^L P(S_\gamma^l | H_\gamma^l) \exp \left[ -\sum_{l,l',\gamma\gamma'} iQ_{\gamma\gamma'}^{l,l'} S_\gamma^l S_{\gamma'}^{l'} \right] \\ &\times \frac{1}{\sqrt{(2\pi)^{2^n L} |\mathbf{C}|}} \exp \left[ -\frac{1}{2} \mathbf{H}^\top \mathbf{C}^{-1} \mathbf{H} \right], \end{aligned} \quad (\text{S17})$$

where  $\mathbf{H} \in \mathbb{R}^{2^n L}$  expresses the pre-activation fields of all patterns and all layers, while  $\mathbf{C}$  is a  $2^n L \times 2^n L$  covariance matrix.

The corresponding saddle point equations are

$$iQ_{\gamma\gamma'}^{l-1,l'-1} = -\sum_n P(n) \frac{\int d\mathbf{H} \sum_{\mathbf{S}} \frac{\partial}{\partial q_{\gamma\gamma'}^{l-1,l'-1}} \mathcal{M}_m(\mathbf{H}, \mathbf{S})}{\int d\mathbf{H} \sum_{\mathbf{S}} \mathcal{M}_m(\mathbf{H}, \mathbf{S})}, \quad 1 \leq l, l' \leq L, \quad (\text{S18})$$

$$iQ_{\gamma\gamma'}^{L,l} = 0, \quad \forall l \quad (\text{S19})$$

$$q_{\gamma\gamma'}^{l,l'} = \sum_m P(m) \langle S_\gamma^l S_{\gamma'}^{l'} \rangle_{\mathcal{M}_m}, \quad 0 \leq l \leq L. \quad (\text{S20})$$



All conjugate order parameters  $\{iQ_{\gamma\gamma'}^{l,l'}\}$  vanish identically similar to the previous case, such that the effective single-site measure becomes

$$\begin{aligned} \mathcal{M}_m(\mathbf{H}, \mathbf{S}) &= \prod_{\gamma=1}^{2^n} P(S_\gamma^0 | S_{m,\gamma}^I) \prod_{l=1}^L P(S_\gamma^l | H_\gamma^l) \\ &\times \frac{1}{\sqrt{(2\pi)^{2nL} |\mathbf{C}|}} \exp \left[ -\frac{1}{2} \mathbf{H}^\top \mathbf{C}^{-1} \mathbf{H} \right], \end{aligned} \quad (\text{S21})$$

and the saddle point equation of the order parameters follows

$$q_{\gamma\gamma'}^{0,0} = \sum_m P(m) S_{m,\gamma}^I S_{m,\gamma'}^I, \quad (\text{S22})$$

$$\begin{aligned} q_{\gamma\gamma'}^{l,0} &= \sum_m P(m) \langle S_\gamma^l S_{\gamma'}^0 \rangle_{\mathcal{M}_m} \\ &= \left( \sum_m P(m) S_{m,\gamma'}^I \right) \int dH_\gamma^l \frac{\phi^l(H_\gamma^l)}{\sqrt{2\pi\sigma_w^2}} \exp \left[ -\frac{1}{2\sigma_w^2} (H_\gamma^l)^2 \right], \end{aligned} \quad (\text{S23})$$

$$q_{\gamma\gamma'}^{l,l'} = \int dH_\gamma^l dH_{\gamma'}^{l'} \frac{\phi^l(H_\gamma^l) \phi^{l'}(H_{\gamma'}^{l'})}{\sqrt{(2\pi)^2 |\Sigma_{\gamma\gamma'}^{l,l'}|}} \exp \left[ -\frac{1}{2} [H_\gamma^l, H_{\gamma'}^{l'}] \cdot (\Sigma_{\gamma\gamma'}^{l,l'})^{-1} \cdot [H_\gamma^l, H_{\gamma'}^{l'}]^\top \right], \quad (\text{S24})$$

where the  $2 \times 2$  covariance matrix  $\Sigma_{\gamma\gamma'}^{l,l'}$  is defined as

$$\Sigma_{\gamma\gamma'}^{l,l'} := \sigma_w^2 \begin{pmatrix} q_{\gamma\gamma}^{l-1,l-1} & q_{\gamma\gamma'}^{l-1,l'-1} \\ q_{\gamma'\gamma}^{l'-1,l-1} & q_{\gamma'\gamma'}^{l'-1,l'-1} \end{pmatrix}. \quad (\text{S25})$$

Similar formalism was derived in the context of dynamical recurrent neural networks to study the autocorrelation of spin/neural dynamics [2].

### C. Strong Equivalence Between Layered and Recurrent Architectures for Odd Activation Functions

In general, the statistical properties of the activities of machines of layered architectures and recurrent architectures are different, since the fields  $\{\mathbf{H}^l\}$  of different layers are directly correlated in the latter case. However, one can observe that the equal-layer overlaps  $q_{\gamma\gamma'}^{l,l}$  in the recurrent architectures is identical to  $q_{\gamma\gamma'}^l$  in the layered architectures, by noticing the same initial condition in Eq. (S22) and Eq. (S11) and the same forward propagation rules in Eq. (S24) (with  $l' = l$ ) and Eq. (S12).

If the cross-layer overlaps  $\{q_{\gamma\gamma'}^{l,l'} | l \neq l'\}$  vanish, then the direct correlation between  $\mathbf{H}^l$  of different layers also vanish such that

$$\frac{1}{\sqrt{(2\pi)^{2nL} |\mathbf{C}|}} \exp \left[ -\frac{1}{2} \mathbf{H}^\top \mathbf{C}^{-1} \mathbf{H} \right] = \prod_l \frac{1}{\sqrt{(2\pi)^{2n} |\mathbf{C}^l|}} \exp \left[ -\frac{1}{2} (\mathbf{H}^l)^\top (\mathbf{C}^l)^{-1} \mathbf{H}^l \right]. \quad (\text{S26})$$

In this case, the distributions of the macroscopic trajectories  $\{\mathbf{H}^l, \mathbf{S}^l\}$  of the two architectures are equivalent. One sufficient condition for this to hold is that the activation functions  $\phi^l(\cdot)$  are odd functions satisfying  $\phi^l(-x) = -\phi^l(x)$ . Firstly, this condition implies that  $q_{\gamma\gamma'}^{l,0} = 0, \forall l$  by Eq. (S23); secondly,  $q_{\gamma\gamma'}^{l,0} = 0$  and the fact that  $\phi^l(\cdot)$  is odd implies  $q_{\gamma\gamma'}^{l+1,1} = 0$ , which leads to  $q_{\gamma\gamma'}^{l,l'} = 0, \forall l \neq l'$  by induction.

### D. Weak Equivalence Between Layered and Recurrent Architectures for General Activation Functions

As shown above, in general the trajectories  $\{\mathbf{H}^l, \mathbf{S}^l\}$  of layered architectures with layer-independent weights follow a different distribution from the case of recurrent architectures with layer-dependent weights except for some specific cases such as DNNs with odd activation functions. Here we focus on the distribution of activities in the output layer.

For layer-dependent weights, the joint distribution of the local fields and activations at layer  $L$  is obtained by marginalize the variables of initial and hidden layers

$$\begin{aligned}
P(\mathbf{H}^L, \mathbf{S}^L) &= \int \prod_{\gamma} \frac{dx_{\gamma}^L}{2\pi} \int \prod_{l=1}^{L-1} \prod_{\gamma} dH_{\gamma}^l \sum_m P(m) \sum_{\{S_{\gamma}^l\}_{\forall \gamma, l < L}} \mathcal{M}_m(\mathbf{H}, \mathbf{S}) \\
&= \int \prod_{l=1}^{L-1} d\mathbf{H}^l \sum_{\{S_{\gamma}^l\}_{\forall \gamma, l < L}} \left( \prod_{l=1}^L \prod_{\gamma} P(S_{\gamma}^l | H_{\gamma}^l) \right) \prod_{l=1}^L \frac{1}{\sqrt{(2\pi)^{2^n} |\mathbf{C}^l|}} \exp \left[ -\frac{1}{2} (\mathbf{H}^l)^{\top} (\mathbf{C}^l)^{-1} \mathbf{H}^l \right] \\
&= \mathcal{N}(\mathbf{H}^L | \mathbf{0}, \mathbf{C}^L(\mathbf{q}^{L-1})) \prod_{\gamma=1}^{2^n} P(S_{\gamma}^L | H_{\gamma}^L), \tag{S27}
\end{aligned}$$

where  $\mathcal{N}(\mathbf{H}^L | \mathbf{0}, \mathbf{C}^L(\mathbf{q}^{L-1}))$  is a  $2^n$  dimensional multivariate Gaussian distribution.

For layer-independent weights, the fields of all layers  $\{\mathbf{H}^l\}$  are coupled with covariance  $\mathbf{C}$

$$\begin{aligned}
P(\mathbf{H}^L, \mathbf{S}^L) &= \int \prod_{l=1}^{L-1} d\mathbf{H}^l \sum_{\{S_{\gamma}^l\}_{\forall \gamma, l < L}} \left( \prod_{l=1}^L \prod_{\gamma} P(S_{\gamma}^l | H_{\gamma}^l) \right) \frac{1}{\sqrt{(2\pi)^{2^n L} |\mathbf{C}|}} \exp \left[ -\frac{1}{2} (\mathbf{H}^{1:L})^{\top} \mathbf{C}^{-1} \mathbf{H}^{1:L} \right] \\
&= \prod_{\gamma} P(S_{\gamma}^L | H_{\gamma}^L) \int \prod_{l=1}^{L-1} d\mathbf{H}^l \frac{1}{\sqrt{(2\pi)^{2^n L} |\mathbf{C}|}} \exp \left[ -\frac{1}{2} (\mathbf{H}^{1:L})^{\top} \mathbf{C}^{-1} \mathbf{H}^{1:L} \right] \\
&= \prod_{\gamma} P(S_{\gamma}^L | H_{\gamma}^L) \frac{1}{\sqrt{(2\pi)^{2^n} |\mathbf{C}^{L,L}|}} \exp \left[ -\frac{1}{2} (\mathbf{H}^L)^{\top} (\mathbf{C}^{L,L})^{-1} \mathbf{H}^L \right] \\
&= \mathcal{N}(\mathbf{H}^L | \mathbf{0}, \mathbf{C}^{L,L}(\mathbf{q}^{L-1, L-1})) \prod_{\gamma=1}^{2^n} P(S_{\gamma}^L | H_{\gamma}^L), \tag{S28}
\end{aligned}$$

where the vector  $\mathbf{H}^{1:L} \in \mathbb{R}^{2^n L}$  is defined as  $\mathbf{H}^{1:L} := (H_1^1, H_2^1, \dots, H_{2^n}^1, H_1^2, H_2^2, \dots, H_{2^n}^2, \dots, H_1^L, H_2^L, \dots, H_{2^n}^L)$ . Since the equal-layer overlap follows the same dynamical rule with the case of layer-dependent weights, the distributions of the two scenarios are equivalent. This suggests that if only the input-output mapping is of interest (but not the hidden layer activity), the activities of the final layer of the two architectures are equivalent.

### III. BOOLEAN FUNCTIONS COMPUTED BY RANDOM DNNS

To examine the distribution of Boolean functions computed at layer  $L$  (we always apply sign activation function in the final layer), notice that nodes at layer  $L$  are not coupled together, so it is sufficient to consider a particular node in the final layer, which follows the distribution of the effective single site measure established before.

Further notice that the local field  $\mathbf{H}^L \in \mathbb{R}^{2^n}$  in the final layer follows a multivariate Gaussian distribution with zero mean and covariance  $\mathbf{C}_{\gamma\gamma'}^L = \sigma_w^2 q_{\gamma\gamma'}^{L-1}$ . Essentially the local field  $H^L$  is a Gaussian process with a dot product kernel (in the limit  $N \rightarrow \infty$ ) [3, 4]

$$k(\vec{x}, \vec{x}') = k\left(\frac{\vec{x} \cdot \vec{x}'}{n}\right) = \sigma_w^2 q_{x, x'}^{L-1}, \tag{S29}$$

where  $\vec{x}, \vec{x}'$  are  $n$ -dimensional vectors.

The probability of a Boolean function  $F(s_{1,\gamma}, \dots, s_{n,\gamma})$  being computed in the fully connected neural network is

$$\begin{aligned}
P(F) &= \left\langle \frac{1}{N} \sum_i \prod_{\gamma=1}^{2^n} \delta(S_{i,\gamma}^L, F(s_{1,\gamma}, \dots, s_{n,\gamma})) \right\rangle \\
&= \left\langle \prod_{\gamma=1}^{2^n} \delta(S_\gamma^L, F(s_{1,\gamma}, \dots, s_{n,\gamma})) \right\rangle \\
&= \sum_{\{S_\gamma^L\}_{\forall \gamma}} \int d\mathbf{H}^L \mathcal{N}(\mathbf{H}^L | 0, \mathbf{C}^L(\mathbf{q})) \prod_{\gamma=1}^{2^n} P(S_\gamma^L | H_\gamma^L) \delta(S_\gamma^L, F(s_{1,\gamma}, \dots, s_{n,\gamma})) \\
&= \int d\mathbf{H}^L \mathcal{N}(\mathbf{H}^L | 0, \mathbf{C}^L(\mathbf{q})) \prod_{\gamma=1}^{2^n} \delta(\text{sgn}(H_\gamma^L), F(s_{1,\gamma}, \dots, s_{n,\gamma})). \tag{S30}
\end{aligned}$$

We focus on systems of layered architectures, where the overlap  $q_{\gamma\gamma'}^l$  is governed by the forward dynamics

$$q_{\gamma\gamma'}^l = \int dH_\gamma^l dH_{\gamma'}^l \frac{\phi(H_\gamma^l) \phi(H_{\gamma'}^l)}{\sqrt{(2\pi)^2 |\Sigma_l|}} \exp \left[ -\frac{1}{2} [H_\gamma^l, H_{\gamma'}^l] \cdot (\Sigma_{\gamma\gamma'}^l (q^{l-1}))^{-1} \cdot [H_\gamma^l, H_{\gamma'}^l]^\top \right]. \tag{S31}$$

- For sign activation function, choosing  $\sigma_w = 1$  yields

$$\Sigma_{\gamma\gamma'}^l = \begin{pmatrix} 1 & q_{\gamma\gamma'}^{l-1} \\ q_{\gamma\gamma'}^{l-1} & 1 \end{pmatrix}, \tag{S32}$$

$$q_{\gamma\gamma'}^l = \frac{2}{\pi} \sin^{-1}(q_{\gamma\gamma'}^{l-1}), \quad \forall l > 0, \tag{S33}$$

$$q_{\gamma\gamma'}^0 = \begin{cases} \frac{1}{n} \sum_{m=1}^n s_{m,\gamma} s_{m,\gamma'}, & \vec{S}^I = \vec{s}, \\ \frac{1}{n+1} \sum_{m=1}^n (1 + s_{m,\gamma} s_{m,\gamma'}). & \vec{S}^I = (\vec{s}, 1). \end{cases} \tag{S34}$$

- For ReLU activation function, choosing  $\sigma_w = \sqrt{2}$  yields

$$\Sigma_{\gamma\gamma'}^l = 2 \begin{pmatrix} q_{\gamma\gamma}^{l-1} & q_{\gamma\gamma'}^{l-1} \\ q_{\gamma\gamma'}^{l-1} & q_{\gamma'\gamma'}^{l-1} \end{pmatrix} = 2 \begin{pmatrix} q_{\gamma\gamma}^{l-1} & q_{\gamma\gamma'}^{l-1} \\ q_{\gamma\gamma'}^{l-1} & q_{\gamma'\gamma'}^{l-1} \end{pmatrix}, \tag{S35}$$

$$q_{\gamma\gamma}^l = \frac{1}{2} \Sigma_{\gamma\gamma}^l = 1, \quad \forall l, \gamma \tag{S36}$$

$$\begin{aligned}
q_{\gamma\gamma'}^l &= \frac{1}{2\pi} \left[ \sqrt{|\Sigma_{\gamma\gamma'}^l|} + \frac{\pi}{2} \Sigma_{\gamma\gamma',12}^l + \Sigma_{\gamma\gamma',12}^l \tan^{-1} \left( \Sigma_{\gamma\gamma',12}^l / \sqrt{|\Sigma_{\gamma\gamma'}^l|} \right) \right] \\
&= \frac{1}{\pi} \left[ \sqrt{1 - (q_{\gamma\gamma'}^{l-1})^2} + q_{\gamma\gamma'}^{l-1} \left( \frac{\pi}{2} + \sin^{-1}(q_{\gamma\gamma'}^{l-1}) \right) \right], \forall l > 0, \tag{S37}
\end{aligned}$$

$$q_{\gamma\gamma'}^0 = \begin{cases} \frac{1}{n} \sum_{m=1}^n s_{m,\gamma} s_{m,\gamma'}, & \vec{S}^I = \vec{s}, \\ \frac{1}{n+1} \sum_{m=1}^n (1 + s_{m,\gamma} s_{m,\gamma'}). & \vec{S}^I = (\vec{s}, 1). \end{cases} \tag{S38}$$

The iteration mappings of overlaps of the two activation functions considered are depicted in Fig. S1.

### A. ReLU Networks in the Large $L$ Limit

In this section, we focus on the large depth limit  $L \rightarrow \infty$ . For ReLU activation function, all the matrix elements of  $\mathbf{C}^L$  become identical in the large  $L$  limit, leading to  $\mathbf{C}^L(\mathbf{q}) \propto J$  (where  $J$  is the all-one matrix) and a degenerate

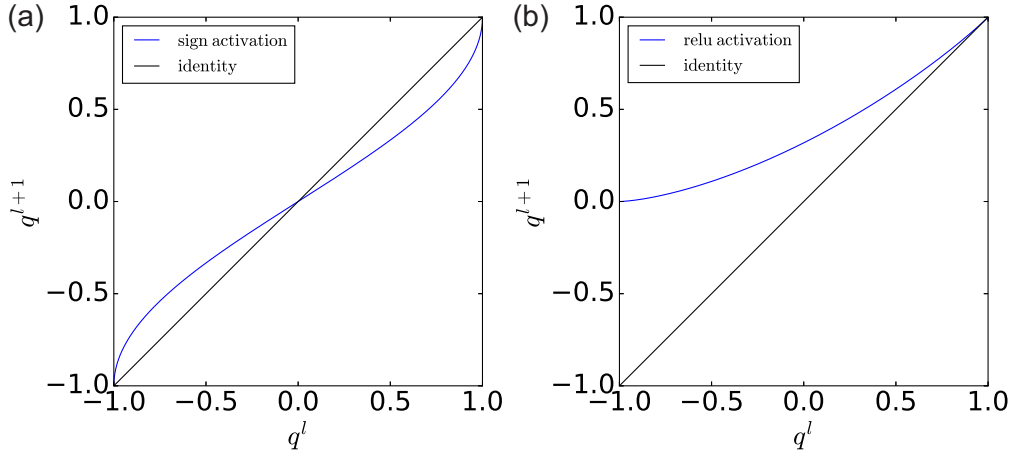


Figure S1. Iteration mappings of overlaps of fully-connected neural networks in the absence of bias variables. (a) sign activation function.  $q^l = 0$  is a stable fixed point while  $q^l = 1, -1$  are two unstable fixed points. (b) ReLU activation functions with  $\sigma_w = \sqrt{2}$ .  $q^l = 1$  is a stable fixed point.

Gaussian distribution of the vector  $\mathbf{H}^L$  enforcing all its components to be the same. To make it explicit, we consider the distribution of  $\mathbf{H}^L$  as follows

$$\begin{aligned} P(\mathbf{H}^L) &= \frac{1}{\sqrt{(2\pi)^M |\mathbf{C}^L|}} \exp \left[ -\frac{1}{2} (\mathbf{H}^L)^\top (\mathbf{C}^L)^{-1} \mathbf{H}^L \right], \\ &= \int \frac{d\mathbf{x}^L}{(2\pi)^M} \exp \left( i\mathbf{x}^L \cdot \mathbf{H}^L - \frac{\sigma_w^2}{2} (\mathbf{x}^L)^\top J \mathbf{x}^L \right) \end{aligned} \quad (\text{S39})$$

$$= \lim_{\kappa \rightarrow 1} \int \frac{d\mathbf{x}^L}{(2\pi)^M} \exp \left( i\mathbf{x}^L \cdot \mathbf{H}^L - \frac{\sigma_w^2}{2} \left[ \sum_{\gamma} (x_{\gamma}^L)^2 + \kappa \sum_{\gamma \neq \gamma'} x_{\gamma}^L x_{\gamma'}^L \right] \right), \quad (\text{S40})$$

Now define  $\mathbf{C}(\kappa) = \sigma_w^2 [(1 - \kappa)I + \kappa J]$  and notice

$$[\mathbf{C}(\kappa)]^{-1} = \frac{1}{\sigma_w^2 (1 - \kappa)} \left( I - \frac{\kappa}{M\rho + (1 - \kappa)} J \right) \approx \frac{1}{\sigma_w^2 (1 - \kappa)} \left( I - \frac{1}{M} J + \frac{1 - \kappa}{M^2 \kappa} J \right), \quad (\text{S41})$$

$$\begin{aligned} P(\mathbf{H}^L) &= \lim_{\kappa \rightarrow 1} \frac{1}{\sqrt{(2\pi)^M |\mathbf{C}(\kappa)|}} \exp \left( -\frac{1}{2} (\mathbf{H}^L)^\top [\mathbf{C}(\kappa)]^{-1} \mathbf{H}^L \right) \\ &= \lim_{\kappa \rightarrow 1} \frac{1}{\sqrt{(2\pi)^M |\mathbf{C}(\kappa)|}} \exp \left\{ -\frac{1}{2} \frac{M}{\sigma_w^2 (1 - \kappa)} \left( \frac{1}{M} \sum_{\gamma} (H_{\gamma}^L)^2 - \left( \frac{1}{M} \sum_{\gamma} H_{\gamma}^L \right)^2 \right) \right\} \\ &\quad \times \exp \left\{ -\frac{1}{2\sigma_w^2 \kappa} \left( \frac{1}{M} \sum_{\gamma} H_{\gamma}^L \right)^2 \right\}. \end{aligned} \quad (\text{S42})$$

In the limit  $\kappa \rightarrow 1$ ,  $P(\mathbf{H}^L)$  has support only in the subspace with  $\frac{1}{M} \sum_{\gamma} (H_{\gamma}^L)^2 - \left( \frac{1}{M} \sum_{\gamma} H_{\gamma}^L \right)^2 = 0$ , requiring all  $H_{\gamma}^L$  to be identical.

Therefore, the output node computes a constant Boolean function in the limit  $L \rightarrow \infty$

$$P(F) = \frac{1}{2}, \quad \text{with } F(\cdot) = 1 \text{ or } F(\cdot) = -1. \quad (\text{S43})$$

## B. Sign Networks in the Large $L$ Limit

### 1. Input Vector $\vec{S}^I = (s_1, s_2, \dots, s_n)$

For the input vector  $\vec{S}^I = (s_1, s_2, \dots, s_n)$ , the overlap at layer 0 is computed as

$$q_{\gamma\gamma'}^0 = \frac{1}{n} \sum_{m=1}^n s_{m,\gamma} s_{m,\gamma'}, \quad (\text{S44})$$

which satisfies  $-1 \leq q_{\gamma\gamma'}^0 \leq 1$ ;  $q_{\gamma\gamma'}^0 = 1$  iff  $\gamma = \gamma'$ , while  $q_{\gamma\gamma'}^0 = -1$  iff  $\bar{s}_{\gamma'} = -\bar{s}_{\gamma}$  (input  $\gamma'$  is the negation of input  $\gamma$ ). We label the  $M = 2^n$  patterns according to

$$\gamma = 1 + \sum_{m=1}^n \frac{1 - s_{m,\gamma}}{2} 2^{n-m}, \quad (\text{S45})$$

$$s_{m,\gamma} = 1 - 2 \times \text{mod} \left( \left\lfloor \frac{\gamma - 1}{2^{n-m}} \right\rfloor, 2 \right). \quad (\text{S46})$$

We note that, the mapping from  $\gamma$  to  $s_{m,\gamma}$  is as follows: (i) represent the integer  $\gamma - 1 \in \{0, 1, \dots, M - 1\}$  by its binary string; for example, for  $n = 3$ , the  $M = 8$  configurations are arranged in the ordered  $[000, 001, 010, 011, 100, 101, 110, 111]$ ; (ii) turn the binary variable 0(1) at each site of the binary string into Ising variable  $+1(-1)$  or  $+(-)$ .

Under this convention, for two negating inputs  $\gamma, \gamma'$   $\bar{s}_{\gamma'} = -\bar{s}_{\gamma}$ , the indices satisfied

$$\begin{aligned} \gamma + \gamma' &= 2 + \sum_{m=1}^n \left( \frac{1 - s_{m,\gamma}}{2} + \frac{1 + s_{m,\gamma}}{2} \right) 2^{n-m} \\ &= 2 + 2^n - 1 = M + 1. \end{aligned} \quad (\text{S47})$$

In the large  $L$  limit, all matrix elements of  $\mathbf{C}^L$  vanish except the diagonal terms  $\Sigma_{\gamma\gamma}^L$  and anti-diagonal terms  $\Sigma_{\gamma\gamma'}^L \delta_{\gamma+\gamma', M+1}$ . For instance, for  $n = 2$ , the covariance matrix  $\Sigma^L$  has the following structure

$$\Sigma^L / \sigma_w^2 = \begin{array}{c|cccc} & ++ & +- & -+ & -- \\ \hline ++ & 1 & 0 & 0 & -1 \\ +- & 0 & 1 & -1 & 0 \\ -+ & 0 & -1 & 1 & 0 \\ -- & -1 & 0 & 0 & 1 \end{array}, \quad (\text{S48})$$

which is singular and corresponds to a degenerate Gaussian distribution of  $\mathbf{H}^L$ . Essentially, it implies that the input  $\gamma$  and its negation  $\gamma'$  are anti-correlated in the local fields  $\langle H_{\gamma}^L H_{\gamma'}^L \rangle / \sigma_w^2 = -1$ .

To make the constraints of the degenerate Gaussian distribution explicit, we consider replacing the anti-diagonal elements of  $\mathbf{C}^L$  by  $\kappa$ , make use of the identities in Sec. VI, and take the limit  $\kappa \rightarrow -1$  in the end of the calculation,

$$\begin{aligned} P(\mathbf{H}^L) &= \lim_{\kappa \rightarrow -1} \int \frac{d\mathbf{x}^L}{(2\pi)^M} \exp \left( i\mathbf{x}^L \cdot \mathbf{H}^L - \frac{\sigma_w^2}{2} (\mathbf{x}^L)^\top \cdot A_M(\kappa) \cdot \mathbf{x}^L \right), \\ &= \lim_{\kappa \rightarrow -1} \frac{1}{\sqrt{(2\pi)^M \sigma_w^{2M} (1 - \kappa^2)^{M/2}}} \exp \left( -\frac{1}{2\sigma_w^2} (\mathbf{H}^L)^\top \cdot A_M(\kappa)^{-1} \cdot \mathbf{H}^L \right), \end{aligned} \quad (\text{S49})$$

$$\begin{aligned} (\mathbf{H}^L)^\top A_M(\kappa)^{-1} \mathbf{H}^L &= \frac{1}{1 - \kappa^2} \sum_{\mu, \nu=1}^M H_{\mu}^L H_{\nu}^L (\delta_{\mu\nu} - \kappa \delta_{\mu+\nu, M+1}) \\ &= \frac{1}{1 - \kappa^2} \sum_{\mu, \nu=1}^M \left[ \frac{1}{2} (H_{\mu}^L)^2 + \frac{1}{2} (H_{\nu}^L)^2 - \kappa H_{\mu}^L H_{\nu}^L \right] \delta_{\mu+\nu, M+1} \\ &= \frac{1}{1 - \kappa^2} \sum_{\mu, \nu=1}^M \left[ \frac{1}{2} (H_{\mu}^L + H_{\nu}^L)^2 - (1 + \kappa) H_{\mu}^L H_{\nu}^L \right] \delta_{\mu+\nu, M+1}, \end{aligned} \quad (\text{S50})$$

$$\begin{aligned}
P(\mathbf{H}^L) &= \lim_{\kappa \rightarrow -1} \frac{1}{\sqrt{(2\pi)^{M/2} \sigma_w^M (1 - \kappa^2)^{M/2}}} \exp\left(-\frac{1}{2\sigma_w^2 (1 - \kappa^2)} \sum_{\gamma=1}^{M/2} (H_\gamma^L + H_{M+1-\gamma}^L)^2\right) \\
&\quad \times \frac{1}{\sqrt{(2\pi)^{M/2} \sigma_w^M}} \exp\left(-\frac{1}{2\sigma_w^2 (1 - \kappa)} 2 \sum_{\gamma=1}^{M/2} H_\gamma^L H_{M+1-\gamma}^L\right) \\
&= \prod_{\gamma=1}^{M/2} \left\{ \delta(H_\gamma^L + H_{M+1-\gamma}^L) \frac{1}{\sqrt{2\pi\sigma_w^2}} \exp\left[-\frac{1}{2\sigma_w^2} (H_\gamma^L)^2\right] \right\}. \tag{S51}
\end{aligned}$$

Therefore, the first  $\frac{M}{2}$  fields are independent of each other, while the last  $\frac{M}{2}$  fields have the opposite sign. The probability of a Boolean function  $F$  being computed is

$$\begin{aligned}
P(F) &= \int d\mathbf{H}^L \mathcal{N}(\mathbf{H}^L | 0, \Sigma^L) \prod_{\gamma} \delta(\text{sgn}(H_\gamma^L), F(\vec{S}_\gamma^I)) \\
&= \prod_{\gamma=1}^{M/2} \int dH_\gamma^L \mathcal{N}(H_\gamma^L | 0, \sigma_w^2) \delta(\text{sgn}(H_\gamma^L), F(\vec{S}_\gamma^I)) \delta(\text{sgn}(-H_\gamma^L), F(\vec{S}_{M+1-\gamma}^I)) \\
&= \prod_{\gamma=1}^{M/2} \frac{1}{2} \mathbb{I}(F(\vec{s}_{M+1-\gamma}) = -F(\vec{s}_\gamma)) \\
&= \frac{1}{\sqrt{2^M}} \prod_{\gamma=1}^{M/2} \mathbb{I}(F(-\vec{s}_\gamma) = -F(\vec{s}_\gamma)), \tag{S52}
\end{aligned}$$

where  $\mathbb{I}(\cdot)$  is the indicator function returning 1 if the condition is met and zero otherwise. The space of functions computed is uniformly distributed among all the odd functions (negated inputs lead to negated output). The restriction to odd functions can be understood by the fact that both  $H_i^l(\vec{S}^{l-1}) = \sum_j W_{ij}^l S_j^{l-1}$  and  $\text{sgn}(H_i^l)$  in the forward propagation are odd functions, which imposes a symmetry constraint in the input-output mappings. Such symmetry is broken by the bias in the input vector  $\vec{S}^I = (\vec{s}, 1)$  as is shown in the following section.

## 2. Input Vector $\vec{S}^I = (s_1, s_2, \dots, s_n, 1)$

If we consider the input vector  $\vec{S}^I = (\vec{s}, 1) = (s_1, s_2, \dots, s_n, 1)$ , the overlap at layer 0 is given by

$$q_{\gamma\gamma'}^0 = \frac{1}{n+1} \left( 1 + \sum_{m=1}^n s_{m,\gamma} s_{m,\gamma'} \right), \tag{S53}$$

which satisfies  $-1 < q_{\gamma\gamma'}^0 \leq 1$  and  $q_{\gamma\gamma'}^0 = 1$  iff  $\gamma = \gamma'$ . This choice of input set is equivalent to adding a bias variable in the first layer. For the sign activation function,  $q^l = 0$  is a stable fixed point unless  $q^0 = 1$ . Therefore, in the large  $L$  limit, all off-diagonal matrix elements of the  $2^n$ -dimensional covariance matrix vanish, leading to  $\mathbf{C}^L(\mathbf{q}) \propto I$ , the identity matrix. The distribution of functions computed at the output node is

$$\begin{aligned}
P(F) &= \int d\mathbf{H}^L \mathcal{N}(\mathbf{H}^L | 0, \sigma_w^2 I) \prod_{\gamma} \delta(\text{sgn}(H_\gamma^L), F(\vec{S}_\gamma^I)) \\
&= \prod_{\gamma} \int dH_\gamma^L \mathcal{N}(H_\gamma^L | 0, \sigma_w^2) \delta(\text{sgn}(H_\gamma^L), F(\vec{S}_\gamma^I)) \\
&= \prod_{\gamma=1}^{2^n} \frac{1}{2} = \frac{1}{2^{2^n}} \tag{S54}
\end{aligned}$$

i.e. the uniform distribution over *all* Boolean functions.



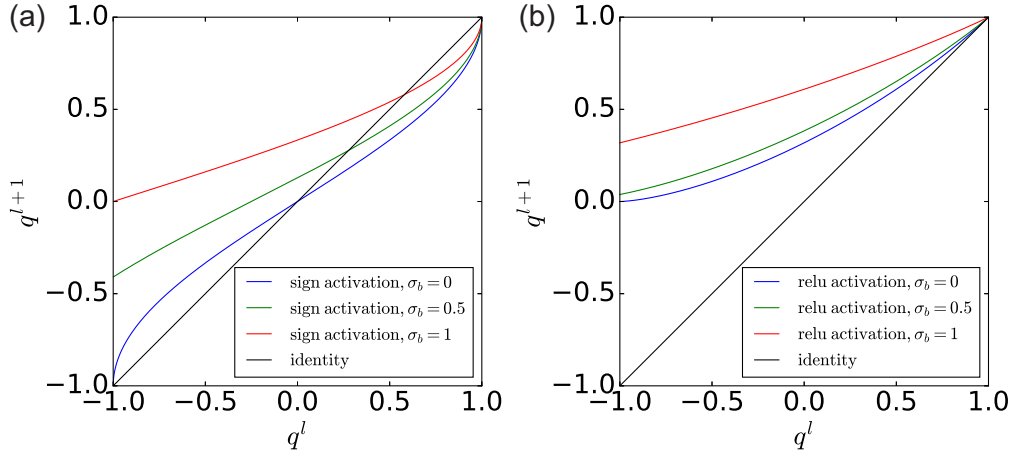


Figure S2. Iteration mappings of overlaps of fully-connected neural networks in the presence of bias variables. (a) sign activation function with  $\sigma_w = 1$ . The overlap  $q^l = 1$  is an unstable fixed point, and there exists a stable fixed point with  $q^* > 0$ . (b) ReLU activation functions with  $\sigma_w^2 = 2 - \sigma_b^2$ .  $q^l = 1$  is a stable fixed point. It shows how the fixed point drifts to a higher value with the increasing bias.

### 3. Introducing Bias Variables

In this section, we introduce the conventional bias variables of neural networks as follows

$$H_i^l(W^l \cdot \bar{S}^{l-1}) = \frac{1}{\sqrt{N}} \sum_{j=1}^N W_{ij}^l S_j^{l-1} + b_i^l, \quad (\text{S55})$$

where  $W_{ij}^l \sim \mathcal{N}(0, \sigma_w^2)$  and  $b_i^l \sim \mathcal{N}(0, \sigma_b^2)$ . The only difference from the case without bias is the average

$$\begin{aligned} & \mathbb{E}_{W,b} \exp \left[ - \sum_{l=1}^L \sum_{\gamma} \sum_{ij} \frac{i}{\sqrt{N}} W_{ij}^l x_{i,\gamma}^l S_{j,\gamma}^{l-1} - \sum_{l=1}^L \sum_{\gamma} \sum_i i x_{i,\gamma}^l b_i^l \right] \\ &= \exp \left[ - \frac{1}{2} \sum_{l=1}^L \sum_{\gamma,\gamma'} \sum_i x_{i,\gamma}^l x_{i,\gamma'}^l \left( \frac{\sigma_w^2}{N} \sum_j S_{j,\gamma}^{l-1} S_{j,\gamma'}^{l-1} + \sigma_b^2 \right) \right]. \end{aligned} \quad (\text{S56})$$

This leads to the following overlap dynamics

- Sign activation

$$q_{\gamma\gamma'}^l = \frac{2}{\pi} \sin^{-1} \left( \frac{\sigma_w^2 q_{\gamma\gamma'}^{l-1} + \sigma_b^2}{\sigma_w^2 + \sigma_b^2} \right), \quad \forall l > 0, \quad (\text{S57})$$

- ReLU activation with  $\sigma_w^2 + \sigma_b^2 = 2$  (to ensure  $q_{\gamma\gamma}^l = 1$ )

$$q_{\gamma\gamma'}^l = \frac{1}{\pi} \left[ \sqrt{1 - \left( \frac{\sigma_w^2 q_{\gamma\gamma'}^{l-1} + \sigma_b^2}{2} \right)^2} + \frac{\sigma_w^2 q_{\gamma\gamma'}^{l-1} + \sigma_b^2}{2} \left( \frac{\pi}{2} + \sin^{-1} \left( \frac{\sigma_w^2 q_{\gamma\gamma'}^{l-1} + \sigma_b^2}{2} \right) \right) \right], \forall l > 0, \quad (\text{S58})$$

The iteration mappings of overlaps considered are depicted in Fig. S2.

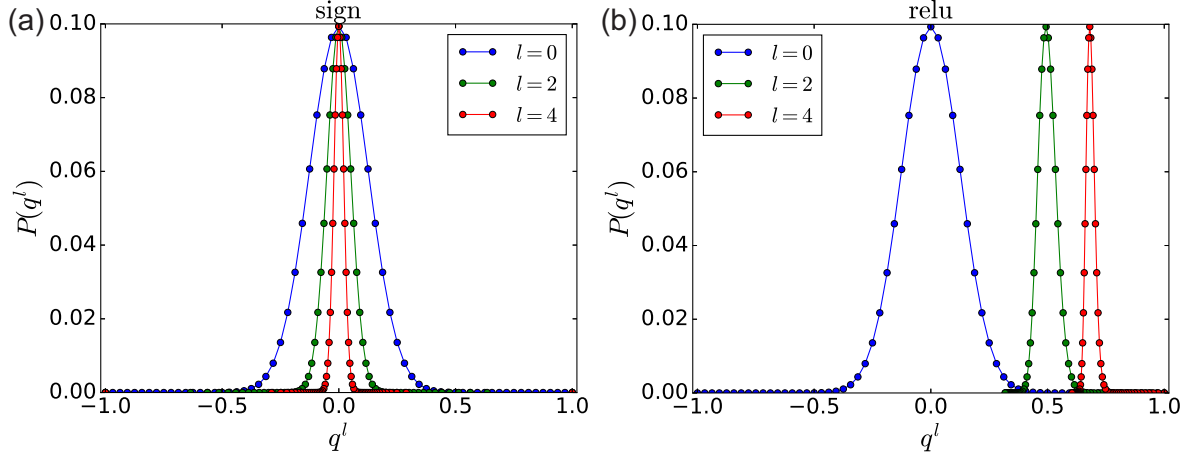


Figure S3. Frequency of appearance of matrix elements  $q^l_{\gamma\gamma'}$  in  $\mathbf{C}^{l+1}$ .  $n = 64$ . (a) Sign activation. (b) ReLU activation.

### C. Finite $L$

Perhaps the more interesting scenario is the case with finite  $L$ . The entropy of the Boolean functions that the output node computes is

$$\begin{aligned}
 \mathcal{H}^L &= - \sum_F P(F) \log P(F) \\
 &= - \sum_{\mathbf{S}^L} P(\mathbf{S}^L) \log P(\mathbf{S}^L) \\
 &= - \sum_{\{\mathbf{S}^L\}_{\forall\gamma}} \int d\mathbf{H}^L \mathcal{N}(\mathbf{H}^L | \mathbf{0}, \mathbf{C}^L) \prod_{\gamma} \delta(S_{\gamma}^L, \text{sgn}(H_{\gamma}^L)) \\
 &\quad \times \log \int d\mathbf{H}^L \mathcal{N}(\mathbf{H}^L | \mathbf{0}, \mathbf{C}^L) \prod_{\gamma} \delta(S_{\gamma}^L, \text{sgn}(H_{\gamma}^L)), \tag{S59}
 \end{aligned}$$

which is fully determined by the covariance matrix  $\mathbf{C}^L(q^{L-1})$ .

For input set of  $\vec{S}^I = (s_1, s_2, \dots, s_n)$ , we have  $q^0_{\gamma\gamma'} \in \{-1, -1 + \frac{2}{n}, \dots, 1\}$ ; the forward propagation rule implies that the overlap  $q^l_{\gamma\gamma'}$  at any layer  $l$  has only  $n + 1$  possible values. The Hamming distance between  $s_{\gamma}^I$  and  $s_{\gamma'}^I$  is  $d_{\gamma\gamma'} = \frac{n}{2}(1 - q^0_{\gamma\gamma'})$ , therefore at each row/column of the matrix  $\mathbf{C}^L$ , there are  $\binom{d_{\gamma\gamma'}}{n}$  elements which take the value  $q^L_{\gamma\gamma'}$ . Fig. S3 depicts the frequency of  $q^l_{\gamma\gamma'}$  in different layers defined as

$$P(q^L) = \binom{d_{\gamma\gamma'}}{n} / 2^n. \tag{S60}$$

Intuitively, the local fields  $H_{\gamma}^L$  that are more correlated lead to a lower entropy of the Boolean functions computed. See Fig. S4 for an illustration of the case of single variable input. It shows a gradual concentration (in layers) around zero of the overlap for sign activation-based layered networks and a concentration while drifting away towards one of the overlap value in the ReLU case. We conjecture that the entropy is monotonically increasing with  $L$  for sign activation function for  $L \geq 1$ , while it is decreasing with ReLU activation functions after the initial increase.

### D. Numerical Computation of Entropy of Functions

In this section we provide some numerical examples of the resulting entropy in different cases. The entropy of  $\mathbf{S}^L$ ,  $\mathcal{H}^L$  is computed according to Eq. (S59); for  $n = 2$ , the entropy can be computed exactly by calculating the orphant probability  $\text{Prob}(H_{\gamma}^L \geq 0)$ ; for  $n > 2$ , we can use Monte Carlo method to sample  $\mathbf{H}^L$  (which is straightforward since

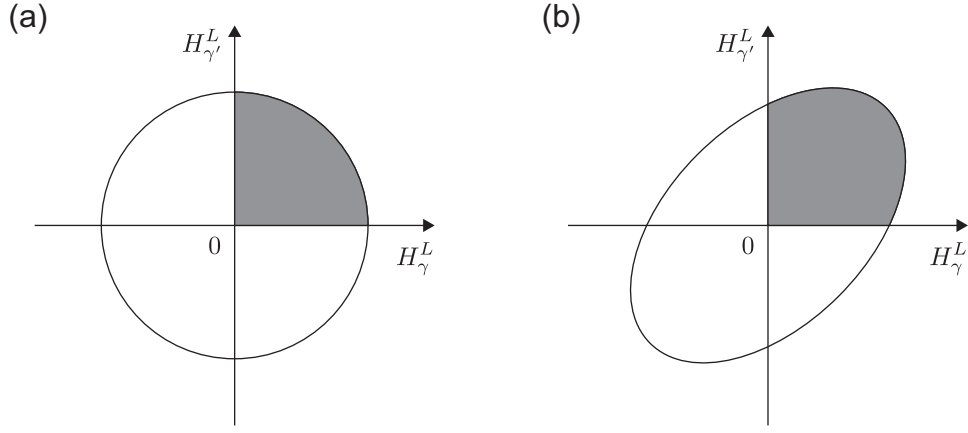


Figure S4. Local field distribution in the case of  $n = 1$ . (a) Uncorrelated Gaussian distribution. The probability mass in the first quadrant corresponds to the function  $F(\cdot) = 1$  being computed with probability  $\frac{1}{4}$ . (b) Correlated Gaussian distribution. The function  $F(\cdot) = 1$  appears with a probability larger than  $\frac{1}{4}$ .

it follows a multivariate Gaussian distribution) and estimate  $\mathcal{H}^L[P(\mathbf{S}^L)]$  accordingly. The obtained entropy  $\mathcal{H}^L$  for neural networks with sign and ReLU activation functions without bias variables are shown in the main text.

#### 1. The Effect of Bias Variables

Without bias variables, the sign-networks are rather chaotic and eventually converge to uniform distribution of all Boolean functions. Introducing bias variables can change the picture, since the local field  $H_i^l = \sum_j W_{ij}^l S_j^{l-1} + b_i^l$  will be less sensitive to the input variables.

In the infinite  $L$  limit, the fixed point of overlap propagation is given by (also see Fig. S2)

$$q_{\gamma\gamma'}^* = \frac{2}{\pi} \sin^{-1} \left( \frac{\sigma_w^2 q_{\gamma\gamma'}^* + \sigma_b^2}{\sigma_w^2 + \sigma_b^2} \right). \quad (\text{S61})$$

So all the off-diagonal matrix elements of  $\mathbf{C}^L$  will converge to the same value  $\sigma_w^2 q^* + \sigma_b^2$ , while all the diagonal matrix elements are  $\sigma_w^2 + \sigma_b^2$ . The entropy of  $\mathbf{H}^L$  and  $\mathbf{S}^L$  is depicted in Fig. S5. The variability of the functions being computed is decreasing with  $\sigma_b$ .

## IV. GENERATING FUNCTIONAL ANALYSIS OF SPARSELY-CONNECTED BOOLEAN CIRCUITS

The analysis in neural networks described above applies similarly to the sparsely-connected Boolean circuits (we use the term circuit to include both layered and recurrent discrete Boolean networks and distinguish them from the real variable networks used before). To accommodate the computation with noise, we consider the output of the  $(l, i)$ -th gate as,

$$S_i^l = \eta_i^l \xi_i^l \alpha_i^l (S_{i_1}^{l-1}, \dots, S_{i_k}^{l-1}) \quad (\text{S62})$$

where  $\eta_i^l$  is an independent random variable from the distribution  $P(\eta) = \epsilon \delta_{\eta; -1} + (1 - \epsilon) \delta_{\eta; 1}$  which represents the *dynamic* (annealed) noise and  $\xi_i^l$  is an independent random variables from the distribution  $P(\xi) = p \delta_{\xi; -1} + (1 - p) \delta_{\xi; 1}$  which represents the *quenched* (hard) noise. We note that the annealed noise is *different* for each copy of the system but the quenched noise (and topology) is the *same* in all copies.

The generating functional is

$$\Gamma[\{\psi_{i,\gamma}^l\}] = \sum_{\{S_{i,\gamma}^l\}_{\gamma=1}^{2^n}} \prod_{l=1}^L P(\vec{S}_\gamma^0 | s_1^\gamma, \dots, s_n^\gamma) \prod_{l=1}^L P(\vec{S}_\gamma^l | \vec{S}_\gamma^{l-1}) e^{-i \sum_{l,i} \psi_{i,\gamma}^l S_{i,\gamma}^l}, \quad (\text{S63})$$

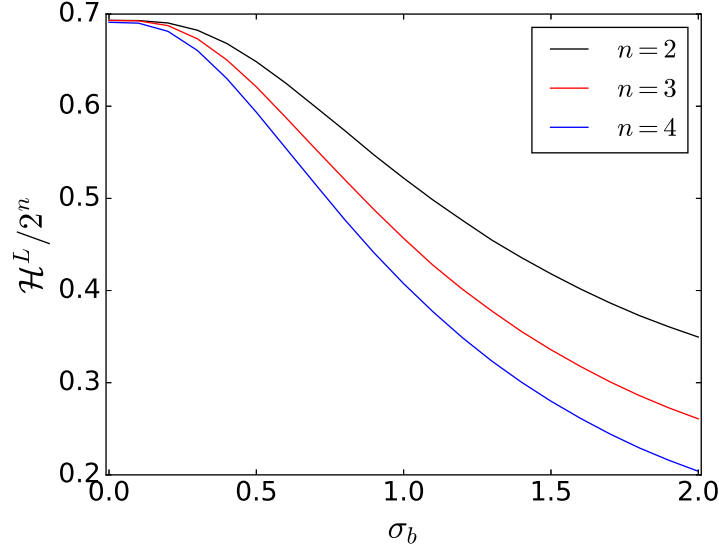


Figure S5. Entropy of Boolean functions vs the variance of bias parameters  $\sigma_b$  in networks with sign activation functions. The variance of weight parameters is  $\sigma_w = 1$ , and the limit  $L \rightarrow \infty$  is considered.

where

$$P(\vec{S}_\gamma^l | \vec{S}_\gamma^{l-1}) = \prod_{i=1}^N \frac{e^{\beta S_{i,\gamma}^l \sum_{j_1, \dots, j_k}^N A_{j_1, \dots, j_k}^{l,i} \xi_i^l \alpha_i^l (S_{j_1, \gamma}^{l-1}, \dots, S_{j_k, \gamma}^{l-1})}}{2 \cosh[\beta \sum_{j_1, \dots, j_k}^N A_{j_1, \dots, j_k}^{l,i} \xi_i^l \alpha_i^l (S_{j_1, \gamma}^{l-1}, \dots, S_{j_k, \gamma}^{l-1})]}. \quad (\text{S64})$$

We have averaged out the noise variables and the inverse temperature  $\beta$  is related to the noise parameter  $\epsilon$  via  $\tanh \beta = 1 - 2\epsilon$ .

The set of connectivity tensors  $\{A_{i_1, \dots, i_k}^{l,i}\}$ , where  $A_{i_1, \dots, i_k}^{l,i} \in \{0, 1\}$ , denotes connections in the circuit. The sources of disorder in our model are the random connections, random boundary conditions and random gates. The former two arise in the layered growth process. The basic change in this growth process is the addition of a new gate with probability  $P(A_{j_1, \dots, j_k}^{l,i}) = \frac{1}{N^k} \delta_{A_{j_1, \dots, j_k}^{l,i}; 1} + (1 - \frac{1}{N^k}) \delta_{A_{j_1, \dots, j_k}^{l,i}; 0}$  of being connected to exactly  $k$  gate-outputs of the previous layer  $l - 1$ . This procedure is carried out independently for all gates in the circuit giving rise to the probability distribution

$$P(\{A_{i_1, \dots, i_k}^{l,i}\}) = \frac{1}{Z_A} \prod_{l,i=1}^{L,N} \left[ \delta \left( 1; \sum_{j_1, \dots, j_k}^N A_{j_1, \dots, j_k}^{l,i} \right) \prod_{i_1, \dots, i_k} \left[ \frac{1}{N^k} \delta_{A_{i_1, \dots, i_k}^{l,i}; 1} + \left( 1 - \frac{1}{N^k} \right) \delta_{A_{i_1, \dots, i_k}^{l,i}; 0} \right] \right], \quad (\text{S65})$$

where  $Z_A$  is a normalization constant. The Kronecker delta function inside the definition (S65) enforces the constraint  $\sum_{j_1, \dots, j_k}^N A_{j_1, \dots, j_k}^{l,i} = 1$ , i.e. the gate on site  $(l, i)$  is mapped to exactly one element from the set of all possible output-indices  $\{i_1, \dots, i_k\}$  from the previous layer.

Random boundary conditions in the layered growth process are generated by selecting indices to the entries of the input vector  $\vec{S}^I$  with probability  $\frac{1}{|\vec{S}^I|}$ , and assigning them to the initial layer  $l = 0$ .

In addition to the topological disorder, induced by the growth process, we assume that the gate  $\alpha_i^l$  added at each step of the process can be sampled randomly and independently from the set  $G$  of  $k$ -ary Boolean gates. Under this assumption the distribution over gates takes the form

$$P(\{\alpha_i^l\}) = \prod_{l=1}^L \prod_{i=1}^N P(\alpha_i^l), \quad (\text{S66})$$

where  $P(\alpha_i^l) = \sum_{\alpha \in G} p_\alpha \delta_{\alpha; \alpha_i^l}$  with  $\sum_{\alpha \in G} p_\alpha = 1$  and  $p_\alpha \geq 0$ . In the simplest case as discussed in the main text, a single gate  $\alpha$  is used with  $P(\alpha_i^l) = \delta_{\alpha; \alpha_i^l}$ .

### A. Layered Architectures

We assume that the system is self-averaging, i.e. any macroscopic quantity which can be computed via Eq. (S63) is self-averaging, and compute the disorder-averaged generating functional

$$\overline{\Gamma[\{\psi_{i,\gamma}^l\}]} = \sum_{\{S_{i,\gamma}^l\}} \prod_{\gamma=1}^{2^n} P(\vec{S}_\gamma^0 | s_1^\gamma, \dots, s_n^\gamma) e^{-i \sum_{l,i} \psi_{i,\gamma}^l S_{i,\gamma}^l} \prod_{\gamma=1}^{2^n} \prod_{l=1}^L \prod_{i=1}^N \frac{e^{\beta S_{i,\gamma}^l H_{i,\gamma}^{l-1}(\vec{S}_\gamma^{l-1})}}{2 \cosh[\beta H_{i,\gamma}^{l-1}(\vec{S}_\gamma^{l-1})]}, \quad (\text{S67})$$

defining the field

$$H_{i,\gamma}^{l-1}(\vec{S}_\gamma^{l-1}) = \sum_{j_1, \dots, j_k} A_{j_1, \dots, j_k}^{l,i} \xi_i^l \alpha_i^l (S_{j_1, \gamma}^{l-1}, \dots, S_{j_k, \gamma}^{l-1}). \quad (\text{S68})$$

Notice that the index convention of the field  $H$  is different from the case of fully-connected neural networks.

Isolating the fields  $\{H_{i,\gamma}^{l-1}(\vec{S}_\gamma^{l-1})\}$  in Eq. (S67) via the integral representations of unity

$$\prod_{\gamma=1}^{2^n} \prod_{l=1}^L \prod_{i=1}^N \left\{ \int \frac{dH_{i,\gamma}^{l-1} dx_{i,\gamma}^{l-1}}{2\pi} e^{ix_{i,\gamma}^{l-1} [H_{i,\gamma}^{l-1} - H_{i,\gamma}^{l-1}(\vec{S}_\gamma^{l-1})]} \right\} = 1 \quad (\text{S69})$$

gives us

$$\begin{aligned} \overline{\Gamma[\{\psi_{i,\gamma}^l\}]} &= \sum_{\{S_{i,\gamma}^l\}} \prod_{\gamma=1}^{2^n} P(\vec{S}_\gamma^0 | s_1^\gamma, \dots, s_n^\gamma) e^{-i \sum_{l,i} \psi_{i,\gamma}^l S_{i,\gamma}^l} \\ &\times \prod_{\gamma=1}^{2^n} \prod_{l=1}^L \prod_{i=1}^N \frac{e^{\beta S_{i,\gamma}^l H_{i,\gamma}^{l-1}}}{2 \cosh \beta H_{i,\gamma}^{l-1}} \int \frac{dH_{i,\gamma}^{l-1} dx_{i,\gamma}^{l-1}}{2\pi} e^{ix_{i,\gamma}^{l-1} H_{i,\gamma}^{l-1}} \\ &\times \prod_{\gamma=1}^{2^n} \prod_{l=1}^L \prod_{i=1}^N e^{-ix_{i,\gamma}^{l-1} \sum_{j_1, \dots, j_k} A_{j_1, \dots, j_k}^{l,i} \xi_i^l \alpha_i^l (S_{j_1, \gamma}^{l-1}, \dots, S_{j_k, \gamma}^{l-1})}. \end{aligned} \quad (\text{S70})$$

We compute the disorder averages in the disorder-dependent part of Eq. (S70) as follows

$$\begin{aligned} &\overline{\prod_{\gamma=1}^{2^n} \prod_{l=1}^L \prod_{i=1}^N \prod_{j_1, \dots, j_k} A_{j_1, \dots, j_k}^{l,i} e^{-ix_{i,\gamma}^{l-1} \sum_{j_1, \dots, j_k} A_{j_1, \dots, j_k}^{l,i} \xi_i^l \alpha_i^l (S_{j_1, \gamma}^{l-1}, \dots, S_{j_k, \gamma}^{l-1})}} \\ &= \frac{1}{Z_A} \prod_{l=1}^L \prod_{i=1}^N \prod_{j_1, \dots, j_k} \left\{ \sum_{A_{i_1, \dots, i_k}^{l,i}} \left[ \frac{1}{N^k} \delta_{A_{i_1, \dots, i_k}^{l,i}; 1} + \left(1 - \frac{1}{N^k}\right) \delta_{A_{i_1, \dots, i_k}^{l,i}; 0} \right] \right\} \delta \left( 1; \sum_{j_1, \dots, j_k} A_{j_1, \dots, j_k}^{l,i} \right) \\ &\times \sum_{\xi_i^l} P(\xi_i^l) \sum_{\alpha_i^l} P(\alpha_i^l) \prod_{\gamma=1}^{2^n} \prod_{j_1, \dots, j_k} e^{-ix_{i,\gamma}^{l-1} \sum_{j_1, \dots, j_k} A_{j_1, \dots, j_k}^{l,i} \xi_i^l \alpha_i^l (S_{j_1, \gamma}^{l-1}, \dots, S_{j_k, \gamma}^{l-1})} \\ &= \frac{1}{Z_A} \prod_{l=1}^L \prod_{i=1}^N \int_{-\pi}^{\pi} \frac{d\omega_i^l}{2\pi} e^{i\omega_i^l} \sum_{\xi_i^l} P(\xi_i^l) \sum_{\alpha_i^l} P(\alpha_i^l) \prod_{i_1, \dots, i_k} \sum_{A_{i_1, \dots, i_k}^{l,i}} \left[ \frac{1}{N^k} \delta_{A_{i_1, \dots, i_k}^{l,i}; 1} + \left(1 - \frac{1}{N^k}\right) \delta_{A_{i_1, \dots, i_k}^{l,i}; 0} \right] \\ &\times e^{-i \sum_{\gamma=1}^{2^n} x_{i,\gamma}^{l-1} \sum_{i_1, \dots, i_k} A_{i_1, \dots, i_k}^{l,i} \xi_i^l \alpha_i^l (S_{i_1, \gamma}^{l-1}, \dots, S_{i_k, \gamma}^{l-1}) - i\omega_i^l \sum_{i_1, \dots, i_k} A_{i_1, \dots, i_k}^{l,i}} \\ &= \frac{1}{Z_A} \prod_{l=1}^L \prod_{i=1}^N \int_{-\pi}^{\pi} \frac{d\omega_i^l}{2\pi} e^{i\omega_i^l} \prod_{i_1, \dots, i_k} \left\langle \frac{1}{N^k} e^{-i \sum_{\gamma=1}^{2^n} x_{i,\gamma}^{l-1} \xi \alpha (S_{i_1, \gamma}^{l-1}, \dots, S_{i_k, \gamma}^{l-1}) - i\omega_i^l} + \left(1 - \frac{1}{N^k}\right) \right\rangle_{\xi, \alpha} \\ &= \frac{1}{Z_A} \prod_{l=1}^L \left\{ \prod_{i=1}^N \int_{-\pi}^{\pi} \frac{d\omega_i^l}{2\pi} e^{i\omega_i^l} \right\} \exp \left[ \frac{1}{N^k} \sum_{i, i_1, \dots, i_k} \left\langle e^{-i \sum_{\gamma=1}^{2^n} x_{i,\gamma}^{l-1} \xi \alpha (S_{i_1, \gamma}^{l-1}, \dots, S_{i_k, \gamma}^{l-1}) - i\omega_i^l} - 1 \right\rangle_{\xi, \alpha} + O(N^{-k+1}) \right] \end{aligned} \quad (\text{S71})$$

Using the result of disorder average in the generating functional Eq. (S70) gives us

$$\begin{aligned}
\bar{\Gamma} &= \frac{1}{Z_A} \sum \prod_{\{S_{i,\gamma}^l\}_{\gamma=1}}^{2^n} P(\vec{S}_\gamma^0 | s_1^\gamma, \dots, s_n^\gamma) e^{-i \sum_{l,i} \psi_{i,\gamma}^l S_{i,\gamma}^l} \\
&\times \left\{ \prod_{l,\gamma,i} \int \frac{dH_{i,\gamma}^l dx_{i,\gamma}^{l-1}}{2\pi} e^{ix_{i,\gamma}^{l-1} H_{i,\gamma}^l} \right\} e^{\beta \sum_{l,\gamma,i} S_{i,\gamma}^l H_{i,\gamma}^{l-1} + \sum_{l,\gamma,i} \log 2 \cosh \beta H_{i,\gamma}^{l-1}} \\
&\times \prod_{l=1}^L \left\{ \prod_{i=1}^N \int_{-\pi}^{\pi} \frac{d\omega_i^l}{2\pi} e^{i\omega_i^l} \right\} \exp \left[ N \int d\mathbf{x} d\omega \frac{1}{N} \sum_{i=1}^N \delta(\mathbf{x} - \mathbf{x}_i^{l-1}) \delta(\omega - \omega_i^l) \right. \\
&\times \left. \sum_{\mathbf{S}_1, \dots, \mathbf{S}_k} \frac{1}{N^k} \sum_{i_1, \dots, i_k} \delta_{\mathbf{S}_1; \mathbf{S}_{i_1}^{l-1}} \times \dots \times \delta_{\mathbf{S}_k; \mathbf{S}_{i_k}^{l-1}} \left\langle e^{-i \sum_{\gamma=1}^{2^n} x_\gamma \xi_\alpha (S_1^\gamma, \dots, S_k^\gamma) - i\omega} - 1 \right\rangle_{\xi, \alpha} + O(N^{-k+1}) \right] \quad (S72)
\end{aligned}$$

where we used the definitions  $\mathbf{x} = (x^1, \dots, x^{2^n})$  and  $\mathbf{S}_j = (S_j^1, \dots, S_j^{2^n})$ , where  $j \in \{1, \dots, k\}$ .

In order to achieve the factorization over sites, we insert the following integro-functional representations of unity

$$\begin{aligned}
&\int \{dP^l d\hat{P}^l\} e^{iN \sum_{\mathbf{S}} \hat{P}^l(\mathbf{S}) [P^l(\mathbf{S}) - \frac{1}{N} \sum_{i=1}^N \delta_{\mathbf{S}; \mathbf{S}_i^l}] } = 1 \\
&\int \{d\Omega^l d\hat{\Omega}^l\} e^{iN \int d\mathbf{x} d\omega \hat{\Omega}^l(\mathbf{x}, \omega) [\Omega^l(\mathbf{x}, \omega) - \frac{1}{N} \sum_{i=1}^N \delta(\mathbf{x} - \mathbf{x}_i^l) \delta(\omega - \omega_i^{l+1})]} = 1
\end{aligned} \quad (S73)$$

into the generating functional Eq. (S72), which leads to

$$\begin{aligned}
\bar{\Gamma} &= \frac{1}{Z_A} \sum \prod_{\{S_{i,\gamma}^l\}_{\gamma=1}}^{2^n} P(\vec{S}_\gamma^0 | s_1^\gamma, \dots, s_n^\gamma) e^{-i \sum_{l,i} \psi_{i,\gamma}^l S_{i,\gamma}^l} \\
&\times \left\{ \prod_{l,\gamma,i} \int \frac{dH_{i,\gamma}^{l-1} dx_{i,\gamma}^{l-1}}{2\pi} e^{ix_{i,\gamma}^{l-1} H_{i,\gamma}^{l-1}} \right\} e^{\beta \sum_{l,\gamma,i} S_{i,\gamma}^l H_{i,\gamma}^{l-1} + \sum_{l,\gamma,i} \log 2 \cosh \beta H_{i,\gamma}^{l-1}} \\
&\times \prod_{l=1}^L \left\{ \prod_{i=1}^N \int_{-\pi}^{\pi} \frac{d\omega_i^l}{2\pi} e^{i\omega_i^l} \right\} \int \{d\Omega^{l-1} d\hat{\Omega}^{l-1}\} e^{iN \int d\mathbf{x} d\omega \hat{\Omega}^{l-1}(\mathbf{x}, \omega) [\Omega^{l-1}(\mathbf{x}, \omega) - \frac{1}{N} \sum_{i=1}^N \delta(\mathbf{x} - \mathbf{x}_i^{l-1}) \delta(\omega - \omega_i^l)]} \\
&\times \int \{dP^{l-1} d\hat{P}^{l-1}\} e^{iN \sum_{\mathbf{S}} \hat{P}^{l-1}(\mathbf{S}) [P^{l-1}(\mathbf{S}) - \frac{1}{N} \sum_{i=1}^N \delta_{\mathbf{S}; \mathbf{S}_i^{l-1}}]} \\
&\times \exp \left[ N \int d\mathbf{x} d\omega \Omega^{l-1}(\mathbf{x}, \omega) \sum_{\mathbf{S}_1, \dots, \mathbf{S}_k} P^{l-1}(\mathbf{S}_1) \times \dots \times P^{l-1}(\mathbf{S}_k) \right. \\
&\times \left. \left\langle e^{-i \sum_{\gamma=1}^{2^n} x_\gamma \xi_\alpha (S_1^\gamma, \dots, S_k^\gamma) - i\omega} - 1 \right\rangle_{\xi, \alpha} + O(N^{-k+1}) \right]. \quad (S74)
\end{aligned}$$

The objective now is to reduce the above equation to a saddle-point integral. This can be achieved if we define two functionals. The first functional is given by

$$\begin{aligned}
\Psi &= -\frac{1}{N} \log Z_A + \sum_{l=0}^{L-1} \left\{ \int d\mathbf{x} d\omega i \hat{\Omega}^l(\mathbf{x}, \omega) \Omega^l(\mathbf{x}, \omega) + \sum_{\mathbf{S}} i \hat{P}^l(\mathbf{S}) P^l(\mathbf{S}) \right. \\
&\quad \left. + \int d\mathbf{x} d\omega \Omega^l(\mathbf{x}, \omega) \sum_{\{\mathbf{S}_j\}_{j=1}^k} \prod_{j=1}^k \{P^l(\mathbf{S}_j)\} \left\langle e^{-i \sum_{\gamma=1}^{2^n} x_\gamma \xi_\alpha (S_1^\gamma, \dots, S_k^\gamma) - i\omega} - 1 \right\rangle_{\xi, \alpha} \right\} \\
&\quad + \frac{1}{N} \sum_{i=1}^N \delta_{m; n_i} \log \sum_{\mathbf{S}_i} \int \{d\mathbf{H}_i d\mathbf{x}_i d\boldsymbol{\omega}_i\} \mathcal{M}_m[\mathbf{S}_i, \mathbf{H}_i | \mathbf{x}_i, \boldsymbol{\omega}_i, \boldsymbol{\psi}_i], \quad (S75)
\end{aligned}$$



and the second functional is given by

$$\begin{aligned} \mathcal{M}_{n_i}[\mathbf{S}_i, \mathbf{H}_i | \mathbf{x}_i, \boldsymbol{\omega}_i, \boldsymbol{\psi}_i] &= \prod_{\gamma=1}^{2^n} \left\{ \delta_{S_{i,\gamma}^0; S_{n_i}^l}(s_1^\gamma, \dots, s_n^\gamma) \right\} e^{-i \sum_{l,\gamma} \psi_{i,\gamma}^l S_{i,\gamma}^l} \\ &\times e^{\sum_{l=0}^{L-1} \sum_{\gamma=1}^{2^n} \{i x_{i,\gamma}^l H_{i,\gamma}^l + \beta S_{i,\gamma}^{l+1} H_{i,\gamma}^l + \log 2 \cosh \beta H_{i,\gamma}^l\}} \\ &\times e^{\sum_{l=0}^{L-1} \{-i \hat{\Omega}^l(\mathbf{x}_i^l, \boldsymbol{\omega}_i^{l+1}) + i \boldsymbol{\omega}_i^{l+1} - i \hat{P}^l(\mathbf{S}_i^l)\}}, \end{aligned} \quad (\text{S76})$$

where we have used the definition

$$\int \{d\mathbf{H}_i d\mathbf{x}_i d\boldsymbol{\omega}_i\} = \prod_{l=0}^{L-1} \left\{ \prod_{\gamma=1}^{2^n} \left\{ \int \frac{dH_{i,\gamma}^l dx_{i,\gamma}^l}{2\pi} \right\} \int_{-\pi}^{\pi} \frac{d\omega_i^{l+1}}{2\pi} \right\}. \quad (\text{S77})$$

Using these definitions in Eq. (S74) gives us the desired saddle-point integral

$$\bar{\Gamma} = \int \{d\boldsymbol{\Omega} d\hat{\boldsymbol{\Omega}} d\mathbf{P} d\hat{\mathbf{P}}\} e^{N\Psi[\boldsymbol{\Omega}, \hat{\boldsymbol{\Omega}}, \mathbf{P}, \hat{\mathbf{P}}]}. \quad (\text{S78})$$

For  $N \rightarrow \infty$  and with the generating fields  $\{\psi_{i,\gamma}^l\}$  are all being set to zero we obtain

$$\begin{aligned} \Psi &= \sum_{l=0}^{L-1} \left\{ i \int d\mathbf{x} d\omega \hat{\Omega}^l(\mathbf{x}, \omega) \Omega^l(\mathbf{x}, \omega) + i \sum_{\mathbf{S}} \hat{P}^l(\mathbf{S}) P^l(\mathbf{S}) \right. \\ &+ \left. \int d\mathbf{x} d\omega \Omega^l(\mathbf{x}, \omega) \sum_{\{\mathbf{S}_j\}} \left\{ \prod_{j=1}^k P^l(\mathbf{S}_j) \right\} \left\langle e^{-i \sum_{\gamma=1}^{2^n} x_\gamma \xi_\alpha(S_1^\gamma, \dots, S_k^\gamma) - i\omega} \right\rangle_{\xi, \alpha} \right\} \\ &+ \sum_m P(m) \log \sum_{\mathbf{S}} \int \{d\mathbf{H} d\mathbf{x} d\boldsymbol{\omega}\} \mathcal{M}_m[\mathbf{S}, \mathbf{H} | \mathbf{x}, \boldsymbol{\omega}, 0]. \end{aligned} \quad (\text{S79})$$

### 1. Saddle-point Problem

The integral Eq. (S78) is dominated by the extremum of the functional Eq. (S79). Functional variation of Eq. (S79) with respect to the integration variables  $\{\boldsymbol{\Omega}, \hat{\boldsymbol{\Omega}}, \mathbf{P}, \hat{\mathbf{P}}\}$  leads us to four saddle-point equations

$$P^l(\mathbf{S}) = \sum_m P(m) \langle \delta_{\mathbf{S}^l; \mathbf{S}} \rangle_{\mathcal{M}_m}, \quad (\text{S80})$$

$$\begin{aligned} \hat{P}^l(\mathbf{S}) &= \frac{\delta}{\delta P^l(\mathbf{S})} \sum_{\{\mathbf{S}_j\}} \prod_{j=1}^k [P^l(\mathbf{S}_j)] \\ &\times \int d\mathbf{x} d\omega \Omega^l(\mathbf{x}, \omega) \left\langle e^{-i \sum_{\gamma=1}^{2^n} x_\gamma \xi_\alpha(S_1^\gamma, \dots, S_k^\gamma) - i\omega} \right\rangle_{\xi, \alpha}, \end{aligned} \quad (\text{S81})$$

$$\Omega^l(\mathbf{x}, \omega) = \sum_m P(m) \langle \delta(\mathbf{x} - \mathbf{x}^l) \delta(\omega - \omega^{l+1}) \rangle_{\mathcal{M}_m}, \quad (\text{S82})$$

$$\hat{\Omega}^l(\mathbf{x}, \omega) = i \sum_{\{\mathbf{S}_j\}} \prod_{j=1}^k \{P^l(\mathbf{S}_j)\} \left\langle e^{-i \sum_{\gamma=1}^{2^n} x_\gamma \xi_\alpha(S_1^\gamma, \dots, S_k^\gamma) - i\omega} \right\rangle_{\xi, \alpha}. \quad (\text{S83})$$

Inserting the result Eq. (S83) into Eq. (S76) and integrating continuous variables leads to

$$\begin{aligned}
& \int \{d\mathbf{H}d\mathbf{x}d\boldsymbol{\omega}\} \mathcal{M}_m[\mathbf{S}, \mathbf{H}|\mathbf{x}, \boldsymbol{\omega}, 0] \\
&= \prod_{\gamma=1}^{2^n} \left\{ \delta_{S_\gamma^0; S_m^I(s_1^\gamma, \dots, s_n^\gamma)} \right\} \int \{d\mathbf{H}d\mathbf{x}d\boldsymbol{\omega}\} \prod_{l=0}^{L-1} e^{\sum_{\gamma=1}^{2^n} \{ix_\gamma^l H_\gamma^l + \beta S_\gamma^{l+1} H_\gamma^l + \log 2 \cosh \beta H_\gamma^l\}} e^{-i\hat{P}^l(\mathbf{S}^l)} \\
&\quad \times \exp \left[ \sum_{\{\mathbf{S}_j\}} \left\{ \prod_{j=1}^k P^l(\mathbf{S}_j) \right\} \left\langle e^{-i\sum_{\gamma=1}^{2^n} x_\gamma^l \xi \alpha(S_1^\gamma, \dots, S_k^\gamma) - i\omega^{l+1}} \right\rangle_{\xi, \alpha} + i\omega^{l+1} \right] \\
&= \prod_{\gamma=1}^{2^n} \left\{ \delta_{S_\gamma^0; S_m^I(s_1^\gamma, \dots, s_n^\gamma)} \right\} \int \{d\mathbf{H}d\mathbf{x}\} \prod_{l=0}^{L-1} e^{\sum_{\gamma=1}^{2^n} \{ix_\gamma^l H_\gamma^l + \beta S_\gamma^{l+1} H_\gamma^l + \log 2 \cosh \beta H_\gamma^l\}} e^{-i\hat{P}^l(\mathbf{S}^l)} \\
&\quad \times \sum_{\{\mathbf{S}_j\}} \prod_{j=1}^k \left\{ P^l(\mathbf{S}_j) \right\} \left\langle e^{-i\sum_{\gamma=1}^{2^n} x_\gamma^l \xi \alpha(S_1^\gamma, \dots, S_k^\gamma)} \right\rangle_{\xi, \alpha} \\
&= \prod_{\gamma=1}^{2^n} \left\{ \delta_{S_\gamma^0; S_m^I(s_1^\gamma, \dots, s_n^\gamma)} \right\} \prod_{l=0}^{L-1} \sum_{\{\mathbf{S}_j\}} \prod_{j=1}^k [P^l(\mathbf{S}_j)] \left\langle \prod_{\gamma=1}^{2^n} \frac{e^{\beta S_\gamma^{l+1} \xi \alpha(S_1^\gamma, \dots, S_k^\gamma)}}{2 \cosh \beta \xi \alpha(S_1^\gamma, \dots, S_k^\gamma)} \right\rangle_{\xi, \alpha} e^{-i\sum_{l=0}^{L-1} \hat{P}^l(\mathbf{S}^l)}.
\end{aligned} \tag{S84}$$

Averaging Eq. (S84) over the random-indices disorder  $m$  gives

$$\begin{aligned}
\text{Prob}[\mathbf{S}^L \leftarrow \dots \leftarrow \mathbf{S}^0] &= \sum_m P(m) \left\{ \prod_{\gamma=1}^{2^n} \delta_{S_\gamma^0; S_m^I(s_1^\gamma, \dots, s_n^\gamma)} \right\} \\
&\quad \times \prod_{l=0}^{L-1} \sum_{\{\mathbf{S}_j\}} \left[ \prod_{j=1}^k P^l(\mathbf{S}_j) \right] \left\langle \prod_{\gamma=1}^{2^n} \frac{e^{\beta S_\gamma^{l+1} \xi \alpha(S_1^\gamma, \dots, S_k^\gamma)}}{2 \cosh \beta \xi \alpha(S_1^\gamma, \dots, S_k^\gamma)} \right\rangle_{\xi, \alpha} \\
&\quad \times e^{-i\sum_{l=0}^{L-1} \hat{P}^l(\mathbf{S}^l)} / \text{Norm}_n,
\end{aligned} \tag{S85}$$

where  $\mathbf{S}^l = (S_1^l, \dots, S_{2^n}^l)$ , which is the probability of a path in the space of Boolean functions of  $n$  variables. The conjugate order parameter  $\hat{P}^l$  is a constant for all  $l \in \{0, \dots, L-1\}$  which is canceled by a similar constant in the denominator of Eq. (S85).

From Eq. (S85) we can easily obtain the probability of a Boolean function on the layer  $l+1$

$$P^{l+1}(\mathbf{S}) = \sum_{\{\mathbf{S}_j\}} \left\{ \prod_{j=1}^k P^l(\mathbf{S}_j) \right\} \left\langle \prod_{\gamma=1}^{2^n} \frac{e^{\beta S_\gamma \xi \alpha(S_1^\gamma, \dots, S_k^\gamma)}}{2 \cosh \beta \xi \alpha(S_1^\gamma, \dots, S_k^\gamma)} \right\rangle_{\xi, \alpha}, \tag{S86}$$

where the initial condition is given by

$$P^0(\mathbf{S}) = \sum_m P(m) \prod_{\gamma=1}^{2^n} \left\{ \delta_{S_\gamma; S_m^I(s_1^\gamma, \dots, s_n^\gamma)} \right\}. \tag{S87}$$

Eq. (S86) is the main result of this section.

## B. Recurrent Architectures

In recurrent Boolean networks, both random connections and random gates do not change from layer to layer but remain fixed. This, for all  $l \in \{1, \dots, L\}$ , gives rise to the probabilities

$$P(\{A_{i_1, \dots, i_k}^i\}) = \frac{1}{Z_A} \prod_{i=1}^N \left[ \delta \left( 1; \sum_{j_1, \dots, j_k} A_{j_1, \dots, j_k}^i \right) \prod_{i_1, \dots, i_k} \left[ \frac{1}{N^k} \delta_{A_{i_1, \dots, i_k}^i; 1} + \left( 1 - \frac{1}{N^k} \right) \delta_{A_{i_1, \dots, i_k}^i; 0} \right] \right], \tag{S88}$$

and

$$P(\{\alpha_i\}) = \prod_{i=1}^N P(\alpha_i). \tag{S89}$$

The differences between the random layered and random recurrent topologies are generated in the disorder-dependent part of Eq. (S67). We average out the disorder in Eq. (S67) as follows

$$\begin{aligned}
& \overline{\prod_{i=1}^N \prod_{\gamma=1}^{2^n} \prod_{l=1}^L \prod_{j_1, \dots, j_k}^N e^{-ix_{i,\gamma}^{l-1} A_{j_1, \dots, j_k}^i} \xi_{i,\alpha_i}(S_{j_1, \gamma}^{l-1}, \dots, S_{j_k, \gamma}^{l-1})} \\
&= \frac{1}{Z_A} \prod_{i=1}^N \prod_{i_1, \dots, i_k}^N \left\{ \sum_{A_{i_1, \dots, i_k}^i} \left[ \frac{1}{N^k} \delta_{A_{i_1, \dots, i_k}^i; 1} + \left(1 - \frac{1}{N^k}\right) \delta_{A_{i_1, \dots, i_k}^i; 0} \right] \right\} \delta\left(1; \sum_{j_1, \dots, j_k}^N A_{j_1, \dots, j_k}^i\right) \\
&\quad \times \sum_{\xi_i} P(\xi_i) \sum_{\alpha_i} P(\alpha_i) \prod_{j_1, \dots, j_k}^N e^{-i \sum_{l=1}^L \sum_{\gamma=1}^{2^n} x_{i,\gamma}^{l-1} A_{j_1, \dots, j_k}^i \xi_{i,\alpha_i}(S_{j_1, \gamma}^{l-1}, \dots, S_{j_k, \gamma}^{l-1})} \\
&= \frac{1}{Z_A} \prod_{i=1}^N \int_{-\pi}^{\pi} \frac{d\omega_i}{2\pi} e^{i\omega_i} \prod_{i_1, \dots, i_k}^N \sum_{A_{i_1, \dots, i_k}^i} \left[ \frac{1}{N^k} \delta_{A_{i_1, \dots, i_k}^i; 1} + \left(1 - \frac{1}{N^k}\right) \delta_{A_{i_1, \dots, i_k}^i; 0} \right] \\
&\quad \times \left\langle e^{-i \sum_{l=1}^L \sum_{\gamma=1}^{2^n} x_{i,\gamma}^{l-1} A_{i_1, \dots, i_k}^i \xi_{i,\alpha_i}(S_{i_1, \gamma}^{l-1}, \dots, S_{i_k, \gamma}^{l-1}) - i\omega_i A_{i_1, \dots, i_k}^i} \right\rangle_{\xi_i, \alpha_i} \\
&= \frac{1}{Z_A} \prod_{i=1}^N \int_{-\pi}^{\pi} \frac{d\omega_i}{2\pi} e^{i\omega_i} \prod_{i_1, \dots, i_k}^N \left\langle \frac{1}{N^k} e^{-i \sum_{l=1}^L \sum_{\gamma=1}^{2^n} x_{i,\gamma}^{l-1} \xi_{\alpha}(S_{i_1, \gamma}^{l-1}, \dots, S_{i_k, \gamma}^{l-1}) - i\omega_i} + \left(1 - \frac{1}{N^k}\right) \right\rangle_{\xi, \alpha} \\
&= \frac{1}{Z_A} \left\{ \prod_{i=1}^N \int_{-\pi}^{\pi} \frac{d\omega_i}{2\pi} e^{i\omega_i} \right\} \exp \left[ \frac{1}{N^k} \sum_{i, i_1, \dots, i_k}^N \left\langle e^{-i \sum_{l=1}^L \sum_{\gamma=1}^{2^n} x_{i,\gamma}^{l-1} \xi_{\alpha}(S_{i_1, \gamma}^{l-1}, \dots, S_{i_k, \gamma}^{l-1}) - i\omega_i} - 1 \right\rangle_{\xi, \alpha} + O(N^{-k+1}) \right], \quad (\text{S90})
\end{aligned}$$

Using the above result in the generating functional Eq. (S70) we obtain

$$\begin{aligned}
\bar{\Gamma} &= \frac{1}{Z_A} \sum_{\{S_{i,\gamma}^l\}} \prod_{\gamma=1}^{2^n} P(\bar{S}_\gamma^0 | s_1^\gamma, \dots, s_n^\gamma) e^{-i \sum_{l,i} \psi_{i,\gamma}^l S_{i,\gamma}^l} \\
&\quad \times \left\{ \prod_{l,\gamma,i} \int \frac{dH_{i,\gamma}^l dx_{i,\gamma}^l}{2\pi} e^{ix_{i,\gamma}^l H_{i,\gamma}^l} \right\} e^{\beta \sum_{l,\gamma,i} S_{i,\gamma}^l H_{i,\gamma}^{l-1} + \sum_{l,\gamma,i} \log 2 \cosh \beta H_{i,\gamma}^{l-1}} \\
&\quad \times \left\{ \prod_{i=1}^N \int_{-\pi}^{\pi} \frac{d\omega_i}{2\pi} e^{i\omega_i} \right\} \exp \left[ N \int d\mathbf{x}^0 \dots d\mathbf{x}^{L-1} d\omega \frac{1}{N} \sum_{i=1}^N \left( \prod_{l=0}^{L-1} \delta(\mathbf{x}^l - \mathbf{x}_i^l) \right) \delta(\omega - \omega_i) \right] \\
&\quad \times \sum_{\{\mathbf{S}_j^l\}} \frac{1}{N^k} \sum_{i_1, \dots, i_k}^N \left( \prod_{l=0}^{L-1} \delta_{\mathbf{S}_{i_1}^l; \mathbf{S}_{i_1}^l} \times \dots \times \delta_{\mathbf{S}_{i_k}^l; \mathbf{S}_{i_k}^l} \right) \\
&\quad \times \left\langle e^{-i \sum_{l=1}^L \sum_{\gamma=1}^{2^n} x_{i,\gamma}^{l-1} \xi_{\alpha}(S_{i_1, \gamma}^{l-1}, \dots, S_{i_k, \gamma}^{l-1}) - i\omega} - 1 \right\rangle_{\xi, \alpha} + O(N^{-k+1}), \quad (\text{S91})
\end{aligned}$$

where we have defined the following vectors  $\mathbf{x}_i^l = (x_{i,1}^l, \dots, x_{i,2^n}^l)$ ,  $\mathbf{x}^l = (x_1^l, \dots, x_{2^n}^l)$ ,  $\mathbf{S}_i^l = (S_{i,1}^l, \dots, S_{i,2^n}^l)$  and  $\mathbf{S}^l = (S_1^l, \dots, S_{2^n}^l)$ .

In order to attain the factorization over sites we insert into Eq. (S91) the following functional unity representations

$$\begin{aligned}
& \int \{dP d\hat{P}\} e^{iN \sum_{\{s^l\}} \hat{P}(\{s^l\}) [P(\{s^l\}) - \frac{1}{N} \sum_{i=1}^N \prod_{l=0}^{L-1} \delta_{s^l; s_i^l}] } = 1, \quad (\text{S92}) \\
& \int \{d\Omega d\hat{\Omega}\} e^{iN \int \{d\mathbf{x}^l\} d\omega \hat{\Omega}(\{\mathbf{x}^l\}, \omega) [\Omega(\{\mathbf{x}^l\}, \omega) - \frac{1}{N} \sum_{i=1}^N [\prod_{l=0}^{L-1} \delta(\mathbf{x}^l - \mathbf{x}_i^l)] \delta(\omega - \omega_i)] } = 1.
\end{aligned}$$

Inserting above into the generating functional Eq. (S91) we obtain

$$\begin{aligned}
\bar{\Gamma} = & \int \{dP d\hat{P} d\Omega d\hat{\Omega}\} \exp N \left[ i \sum_{\{\mathbf{S}^l\}} \hat{P}(\{\mathbf{S}^l\}) P(\{\mathbf{S}^l\}) + i \int \{d\mathbf{x}^l\} d\omega \hat{\Omega}(\{\mathbf{x}^l\}, \omega) \Omega(\{\mathbf{x}^l\}, \omega) \right. \\
& + \int \{d\mathbf{x}^l\} d\omega \Omega(\{\mathbf{x}^l\}, \omega) \sum_{\{\mathbf{S}_j^l\}} P(\{\mathbf{S}_1^l\}) \times \cdots \times P(\{\mathbf{S}_k^l\}) \times \cdots \\
& \left. \cdots \times \left\langle e^{-i \sum_{l=1}^L \sum_{\gamma=1}^{2^n} x_\gamma^{l-1} \xi_\alpha(S_{1,\gamma}^{l-1}, \dots, S_{k,\gamma}^{l-1}) - i\omega} - 1 \right\rangle_{\xi, \alpha} - \frac{1}{N} \log Z_A \right] \\
& \times \sum_{\{S_{i,\gamma}^l\}_{\gamma=1}^{2^n}} P(\bar{S}_\gamma^0 | s_1^\gamma, \dots, s_n^\gamma) e^{-i \sum_{l,i} \psi_{i,\gamma}^l S_{i,\gamma}^l} \\
& \times \left\{ \prod_{l,\gamma,i} \int \frac{dH_{i,\gamma}^l dx_{i,\gamma}^l}{2\pi} e^{ix_{i,\gamma}^l H_{i,\gamma}^l} \right\} e^{\beta \sum_{l,\gamma,i} S_{i,\gamma}^l H_{i,\gamma}^{l-1} + \sum_{l,\gamma,i} \log 2 \cosh \beta H_{i,\gamma}^{l-1}} \\
& \times \left\{ \prod_{i=1}^N \int_{-\pi}^{\pi} \frac{d\omega_i}{2\pi} e^{i\omega_i} \right\} e^{-i \sum_{i=1}^N \hat{P}(\{\mathbf{S}_i^l\}) - i \sum_{i=1}^N \hat{\Omega}(\{\mathbf{x}_i^l\}, \omega_i)}. \tag{S93}
\end{aligned}$$

The site-dependent part of the above can be written as

$$\exp \left[ N \frac{1}{N} \sum_{i=1}^N \delta_{m;n_i} \log \sum_{\{\mathbf{S}_i^l\}} \int \{d\mathbf{H}_i^l d\mathbf{x}_i^l\} \int_{-\pi}^{\pi} \frac{d\omega_i}{2\pi} \times \cdots \times \mathcal{M}_m[\{\mathbf{S}_i^l\}, \{\mathbf{H}_i^l\} | \{\mathbf{x}_i^l\}, \omega_i, \{\psi_i^l\}] \right], \tag{S94}$$

where

$$\mathcal{M}_{n_i}[\{\mathbf{S}_i^l\}, \{\mathbf{H}_i^l\} | \{\mathbf{x}_i^l\}, \omega_i, \{\psi_i^l\}] = \prod_{\gamma=1}^{2^n} \left\{ \delta_{S_{i,\gamma}^0; S_{n_i}^l(s_1^\gamma, \dots, s_n^\gamma)} \right\} e^{-i \sum_{l,\gamma} \psi_{i,\gamma}^l S_{i,\gamma}^l} \tag{S95}$$

$$\begin{aligned}
& \times e^{\sum_{l=0}^{L-1} \sum_{\gamma=1}^{2^n} \{ix_{i,\gamma}^l H_{i,\gamma}^l + \beta S_{i,\gamma}^{l+1} H_{i,\gamma}^l + \log 2 \cosh \beta H_{i,\gamma}^l\}} \\
& \times e^{-i\hat{\Omega}(\{\mathbf{x}_i^l\}, \omega_i) + i\omega_i - i\hat{P}(\{\mathbf{S}_i^l\})}, \tag{S96}
\end{aligned}$$

and we use the definition  $\int \{d\mathbf{H}_i^l d\mathbf{x}_i^l\} = \prod_{l=0}^{L-1} \prod_{\gamma=1}^{2^n} \int \frac{dH_{i,\gamma}^l dx_{i,\gamma}^l}{2\pi}$ .

The definition Eq. (S94) allows us to express the disorder-averaged generating functional Eq. (S93) as a saddle-point integral

$$\bar{\Gamma} = \int \{dP d\hat{P} d\Omega d\hat{\Omega}\} e^{N\Psi[\{P, \hat{P}, \Omega, \hat{\Omega}\}]} \tag{S97}$$

where

$$\begin{aligned}
\Psi = & \sum_{\{\mathbf{S}^l\}} i\hat{P}(\{\mathbf{S}^l\}) P(\{\mathbf{S}^l\}) + \int \{d\mathbf{x}^l\} d\omega i\hat{\Omega}(\{\mathbf{x}^l\}, \omega) \Omega(\{\mathbf{x}^l\}, \omega) \\
& + \int \{d\mathbf{x}^l\} d\omega \Omega(\{\mathbf{x}^l\}, \omega) \sum_{\{\mathbf{S}_j^l\}} P(\{\mathbf{S}_1^l\}) \times \cdots \times P(\{\mathbf{S}_k^l\}) \times \cdots \\
& \cdots \times \left\langle e^{-i \sum_{l=0}^{L-1} \sum_{\gamma=1}^{2^n} x_\gamma^l \xi_\alpha(S_{1,\gamma}^l, \dots, S_{k,\gamma}^l) - i\omega} - 1 \right\rangle_{\xi, \alpha} - \frac{1}{N} \log Z_A \\
& + \sum_m P(m) \log \sum_{\{\mathbf{S}^l\}} \int \{d\mathbf{H}^l d\mathbf{x}^l\} \int_{-\pi}^{\pi} \frac{d\omega}{2\pi} \mathcal{M}_m[\{\mathbf{S}^l\}, \{\mathbf{H}^l\} | \{\mathbf{x}^l\}, \omega, \{0\}].
\end{aligned} \tag{S98}$$

with

$$\begin{aligned}
\mathcal{M}_m[\{\mathbf{S}^l\}, \{\mathbf{H}^l\} | \{\mathbf{x}^l\}, \omega, \{0\}] = & P_m(\mathbf{S}^0) \prod_{l=0}^{L-1} \frac{e^{\beta \mathbf{S}^{l+1} \cdot \mathbf{H}^l}}{\prod_\gamma 2 \cosh \beta H_\gamma^l} e^{i\mathbf{x}^l \cdot \mathbf{H}^l} \\
& \times e^{-i\hat{\Omega}(\{\mathbf{x}^l\}, \omega) + i\omega - i\hat{P}(\{\mathbf{S}^l\})}
\end{aligned}$$

where  $P_m(\mathbf{S}^0) = \prod_{\gamma=1}^{2^n} \left\{ \delta_{S_\gamma^0; S_m^l(s_\gamma^1, \dots, s_\gamma^n)} \right\}$ ; we have removed the generating fields  $\{\psi_i^l\} = \{0\}$  and assumed the law of large numbers  $P(m) = \lim_{N \rightarrow \infty} \frac{1}{N} \sum_{i=1}^N \delta_{m; n_i}$  holds. For  $N \rightarrow \infty$  the integral Eq. (S97) is dominated by the extremum points of Eq. (S98) i.e.  $\frac{\delta \Psi}{\delta P} = 0$ ,  $\frac{\delta \Psi}{\delta \hat{P}} = 0$ ,  $\frac{\delta \Psi}{\delta \Omega} = 0$  and  $\frac{\delta \Psi}{\delta \hat{\Omega}} = 0$ .

Computing the extremum points of Eq. (S98) leads to the saddle-point equations

$$P(\{\mathbf{S}^l\}) = \sum_m P(m) \left\langle \prod_{l=0}^{L-1} \delta_{\mathbf{S}^l; \mathbf{S}^l} \right\rangle_{\mathcal{M}_m} \quad (\text{S99})$$

$$\begin{aligned} \hat{P}(\{\mathbf{S}^l\}) &= i \frac{\delta}{\delta P(\{\mathbf{S}^l\})} \sum_{\{\mathbf{S}_j^l\}} \prod_{j=1}^k P(\{\mathbf{S}_j^l\}) \int \{d\mathbf{x}^l\} d\omega \Omega(\{\mathbf{x}^l\}, \omega) \\ &\times \left\langle e^{-i \sum_{l=0}^{L-1} \sum_{\gamma=1}^{2^n} x_\gamma^l \xi_\alpha(S_{1,\gamma}^l, \dots, S_{k,\gamma}^l) - i\omega} \right\rangle_{\xi, \alpha} \end{aligned} \quad (\text{S100})$$

$$\Omega(\{\mathbf{x}^l\}, \omega') = \sum_m P(m) \left\langle \left[ \prod_{l=0}^{L-1} \delta(\mathbf{x}^l - \mathbf{x}^l) \right] \delta(\omega' - \omega) \right\rangle_{\mathcal{M}_m} \quad (\text{S101})$$

$$\hat{\Omega}(\{\mathbf{x}^l\}, \omega) = i \sum_{\{\mathbf{S}_j^l\}} \prod_{j=1}^k P(\{\mathbf{S}_j^l\}) \left\langle e^{-i \sum_{l=0}^{L-1} \sum_{\gamma=1}^{2^n} x_\gamma^l \xi_\alpha(S_{1,\gamma}^l, \dots, S_{k,\gamma}^l) - i\omega} \right\rangle_{\xi, \alpha}, \quad (\text{S102})$$

where we use the definition

$$\langle \dots \rangle_{\mathcal{M}_m} = \frac{\sum_{\{\mathbf{S}^l\}} \int \{d\mathbf{H}^l d\mathbf{x}^l\} \int_{-\pi}^{\pi} \frac{d\omega}{2\pi} \mathcal{M}_m[\{\mathbf{S}^l\}, \{\mathbf{H}^l\} | \{\mathbf{x}^l\}, \omega, \{0\}] \dots}{\sum_{\{\mathbf{S}^l\}} \int \{d\mathbf{H}^l d\mathbf{x}^l\} \int_{-\pi}^{\pi} \frac{d\omega}{2\pi} \mathcal{M}_m[\{\mathbf{S}^l\}, \{\mathbf{H}^l\} | \{\mathbf{x}^l\}, \omega, \{0\}]}$$

Solving the saddle point equations leads to the main result

$$P(\mathbf{S}^L, \dots, \mathbf{S}^0) = \sum_m P(m) P_m(\mathbf{S}^0) \sum_{\{\mathbf{S}_j^l\}} \prod_{j=1}^k P(\{\mathbf{S}_j^l\}) \left\langle \prod_{l=0}^{L-1} \prod_{\gamma=1}^{2^n} \frac{e^{\beta S_\gamma^{l+1} \xi_\alpha(S_{1,\gamma}^l, \dots, S_{k,\gamma}^l)}}{2 \cosh \beta \xi_\alpha(S_{1,\gamma}^l, \dots, S_{k,\gamma}^l)} \right\rangle_{\xi, \alpha} \quad (\text{S103})$$

We can use this result to generate: (i) single-layer (time) observables

$$P(\mathbf{S}^L) = \sum_{\mathbf{S}_j^{L-1}} \left\{ \prod_{j=1}^k P(\mathbf{S}_j^{L-1}) \right\} \left\langle \prod_{\gamma=1}^{2^n} \frac{e^{\beta S_\gamma^L \xi_\alpha(S_{1,\gamma}^{L-1}, \dots, S_{k,\gamma}^{L-1})}}{2 \cosh \beta \xi_\alpha(S_{1,\gamma}^{L-1}, \dots, S_{k,\gamma}^{L-1})} \right\rangle_{\xi, \alpha}, \quad (\text{S104})$$

(ii) two-layer (time) observables

$$P(\mathbf{S}^L, \mathbf{S}^{L'}) = \sum_{\{\mathbf{S}_j^{L-1}, \mathbf{S}_j^{L'-1}\}} \prod_{j=1}^k P(\mathbf{S}_j^{L-1}, \mathbf{S}_j^{L'-1}) \left\langle \prod_{\gamma=1}^{2^n} \frac{e^{\beta S_\gamma^L \xi_\alpha(S_{1,\gamma}^{L-1}, \dots, S_{k,\gamma}^{L-1})}}{2 \cosh \beta \xi_\alpha(S_{1,\gamma}^{L-1}, \dots, S_{k,\gamma}^{L-1})} \frac{e^{\beta S_\gamma^{L'} \xi_\alpha(S_{1,\gamma}^{L'-1}, \dots, S_{k,\gamma}^{L'-1})}}{2 \cosh \beta \xi_\alpha(S_{1,\gamma}^{L'-1}, \dots, S_{k,\gamma}^{L'-1})} \right\rangle_{\xi, \alpha} \quad (\text{S105})$$

According to (i) the results for the layered growth process Eq. (S86) also hold for the recurrent topology.

## V. SOME RESULTS OF BOOLEAN CIRCUITS

### A. Savicky's Growth Process

In this section we will use Eq. (S86) to study the Boolean functions generated in the layered variant [5] of the Savicky's growth process [6].

But first we will establish the equivalence of these two growth processes. Assuming that the formulae in our growth process are constructed using only a single gate  $\alpha$  and that it has no noise, we obtain

$$P^{L+1}(\mathbf{S}) = \sum_{\{\mathbf{S}_j\}} \left[ \prod_{j=1}^k P^l(\mathbf{S}_j) \right] \prod_{\gamma=1}^{2^n} \delta[S^\gamma; \alpha(S_1^\gamma, \dots, S_k^\gamma)], \quad (\text{S106})$$

where  $\mathbf{S} \in \{-1, 1\}^{2^n}$ .

This result is in agreement with [6], which establishes a formal equivalence of the layered network and Savicky's formula-growth process.

From [5] and [6, 7] we know that the growth process can converge to a single Boolean function or uniform distribution over some set of all Boolean functions.

### 1. Single Boolean Function

In the case where the process converges to a single Boolean function  $\mathbf{f}$  we have  $P^\infty(\mathbf{S}) = \prod_{\gamma=1}^{2^n} \delta[S^\gamma; f^\gamma]$ , where we represent  $\mathbf{f}$  as a binary string of length  $2^n$ .

Inserting above into Eq. (S106) we obtain

$$\begin{aligned} \prod_{\gamma=1}^{2^n} \delta[S^\gamma; f^\gamma] &= \sum_{\{\mathbf{S}_j\}} \prod_{j=1}^k \left[ \prod_{\gamma=1}^{2^n} \delta[S_j^\gamma; f^\gamma] \right] \prod_{\gamma=1}^{2^n} \delta[S^\gamma; \alpha(S_1^\gamma, \dots, S_k^\gamma)] \\ &= \prod_{\gamma=1}^{2^n} \delta[S^\gamma; \alpha(f^\gamma, \dots, f^\gamma)]. \end{aligned} \quad (\text{S107})$$

Thus, when the process converges to a single Boolean function  $f$  this implies that  $f^\gamma = \alpha(f^\gamma, \dots, f^\gamma)$  and the number of fixed points of Eq. (S106) is equal to  $2^{2^n}$ , i.e. all Boolean functions of  $n$  variables.

In order to find out, for a given gate  $\alpha$  which satisfies the property  $S = \alpha(S, \dots, S)$ , to which Boolean function the growth process converges to (if at all) we have to study the evolution of the probability  $P^l(\mathbf{S})$  which depends on the input set  $S^l$  via  $P^0(\mathbf{S})$ .

The (Shannon) entropy of a Boolean function  $f$  on layer  $l$  is defined as  $H^l = -\sum_{\mathbf{S}} P^l(\mathbf{S}) \log P^l(\mathbf{S})$ , where we use the convention  $P^l(\mathbf{S}) \log P^l(\mathbf{S}) = 0$  when  $P^l(\mathbf{S}) = 0$ . For  $\mathbf{S} \in \{-1, 1\}^{2^n}$ , we have  $0 \leq H^l \leq 2^n \log n$  and  $H^l \leq H_1^l + \dots + H_{2^n}^l$ , where  $H_\gamma^l = -\sum_{S} P_\gamma^l(S) \log P_\gamma^l(S)$ , which implies  $0 \leq H^l \leq H_1^l + \dots + H_{2^n}^l$ .

The marginals  $P_\gamma^l(S) = \frac{1}{2}[1 + S m_\gamma^l]$  of (S106) can be computed from the equation

$$m_\gamma^{l+1} = \sum_{\{\mathbf{S}_j\}} \prod_{j=1}^k \left[ \frac{1 + S_j m_\gamma^l}{2} \right] \alpha(S_1, \dots, S_k), \quad (\text{S108})$$

where  $\gamma = 1, \dots, 2^n$  and  $m_\gamma^0 = \frac{1}{|S^l|} \sum_{S \in S^l(\bar{s})} S$ .

We notice that for  $l \rightarrow \infty$ :  $H_1^l + \dots + H_{2^n}^l = 0$  only when  $m_\gamma^l \in \{-1, 1\}$  for all  $\gamma \in \{1, \dots, 2^n\}$ .

Let  $m_\gamma^l = S$ , where  $S \in \{-1, 1\}$ , and compute RHS of Eq. (S108). The result is given by  $\alpha(S, \dots, S)$ . The convergence of the process to a single Boolean function implies that  $S = \alpha(S, \dots, S)$  which consequently implies that  $m_\gamma^l = \pm 1$  are the fixed points of the dynamics Eq. (S108).

Let  $B_-$  and  $B_+$  be basins of attraction of equation of the fixed points  $-1$  and  $+1$  respectively. For an arbitrary Boolean function  $F : \{-1, 1\}^n \rightarrow \{-1, 1\}$ , define two sets of inputs  $s_\pm$  for which  $F(s_1, \dots, s_n) = \pm 1$  then the process Eq. (S106) converges to the Boolean function  $F$  when for all  $(s_1, \dots, s_n) \in s_\pm$ ,  $m^0 = \frac{1}{|S^l|} \sum_{S \in S^l(\bar{s})} S \in B_\pm$ .

An example of iteration maps of the Eq. (S108) for AND and OR gates is plotted in Fig. (S6)(a). For these gates,  $m_\gamma^l$  always converges to the fixed points  $m^* = \pm 1$  as the number of layers grows, which suggests that the corresponding Boolean circuits compute a single Boolean function in the large depth limit. For MAJ3 gate where the iteration map is plotted in Fig. (S6)(b), if we consider the input vector  $\bar{S}^l = (s_1, \dots, s_n)$ , where  $n$  is odd, then  $m^0 \neq 0$  and  $m_\gamma^l$  converges to the fixed points  $m^* = \pm 1$  as well, i.e a single Boolean function is computed in the large depth limit.

### 2. Uniform Distribution over All Boolean Functions

In the case when the growth process converges to a uniform distribution over all Boolean functions we have  $P^\infty(\mathbf{S}) = \frac{1}{2^{2^n}}$ .



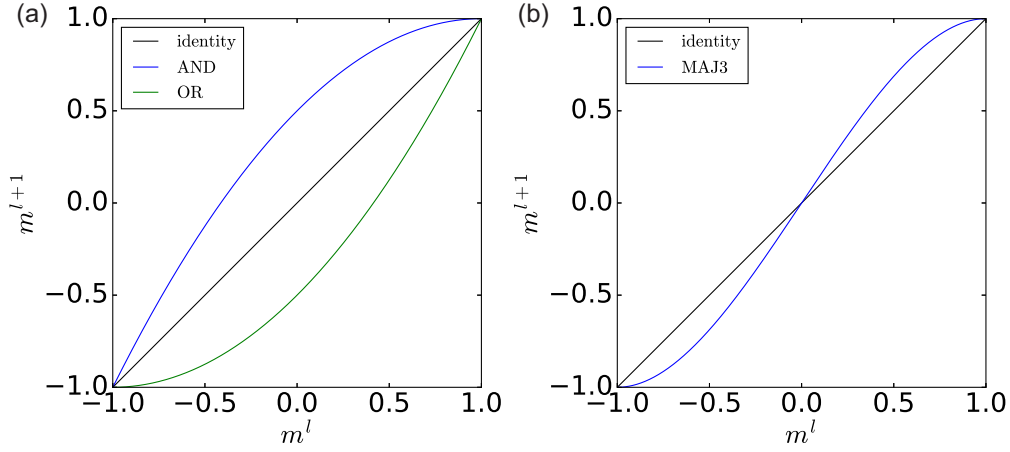


Figure S6. Iteration maps of Eq. (S108). (a) AND and OR gate Boolean circuits;  $m^* = \pm 1$  are the only fixed points of the iteration. (b) MAJ3 gate Boolean circuits;  $m^* = \pm 1$  are stable fixed points, while  $m^* = 0$  is an unstable fixed point.

Inserting this distribution into Eq. (S106) we obtain

$$\begin{aligned}
 \frac{1}{2^{2^n}} &= \sum_{\{S_j\}} \prod_{j=1}^k \left[ \frac{1}{2^{2^n}} \right] \prod_{\gamma=1}^{2^n} \delta[S^\gamma; \alpha(S_1^\gamma, \dots, S_k^\gamma)] \\
 &= \frac{1}{2^{k2^n}} \prod_{\gamma=1}^{2^n} \sum_{S_1, \dots, S_k} \delta[S^\gamma; \alpha(S_1, \dots, S_k)] \\
 &= \frac{1}{2^{k2^n}} \prod_{\gamma=1}^{2^n} \left[ 2^{k-1} + \frac{S^\gamma}{2} \sum_{S_1, \dots, S_k} \alpha(S_1, \dots, S_k) \right]
 \end{aligned} \tag{S109}$$

This equality holds when the gate  $\alpha$  is balanced

$$\sum_{S_1, \dots, S_k} \alpha(S_1, \dots, S_k) = 0. \tag{S110}$$

To show that the process converges to  $P^\infty(\mathbf{S}) = \frac{1}{2^{2^n}}$ , for a given balanced and non-linear [6] gate  $\alpha$ , and initial conditions given by  $P^0$ , we have to study the dynamics of  $P^l$  in general which is beyond the scope of the current study. Note that in the context of Boolean circuits, the variables are always Boolean and linearity is defined in the finite field  $GF(2)$  [6, 7]. The requirement for gate  $\alpha$  to be non-linear is due to the fact that any composition of linear Boolean gates is also linear, which implies that only linear Boolean functions can be represented in Boolean circuits using linear gate  $\alpha$ . Therefore a non-linear gate is required in order to generate all Boolean functions [6].

As an example, the MAJ3 gate  $\alpha(S_1, S_2, S_3) = \text{sgn}(S_1 + S_2 + S_3)$  is balanced and non-linear. If the balanced input  $\vec{S}^I = (\vec{s}, -\vec{s}, 1, -1)$  is used, then  $m_\gamma^0 = 0$ , which implies that  $m_\gamma^l = 0, \forall l \geq 1$ . Numerical evidence in the main text shows that (at least for small values of  $n$ ), the entropy of Boolean functions  $\mathcal{H}^L$  increases monotonically as the number of layers grows and converges to its maximum value  $2^n \log 2$ . It implies that the variability of the Boolean functions computed is increasing and the machines converge to a uniform distribution on all Boolean functions in the large depth limit, which is consistent with the findings in [6].

## VI. IDENTITY MATRIX PLUS ANTI-DIAGONAL MATRIX

Consider the  $M \times M$  matrix  $A_M(\kappa)$  with matrix element

$$A_M(\kappa)_{ij} = \delta_{ij} + \kappa \delta_{i+j, M+1}. \tag{S111}$$

For instance,

$$A_4(\kappa) = \begin{pmatrix} 1 & 0 & 0 & \kappa \\ 0 & 1 & \kappa & 0 \\ 0 & \kappa & 1 & 0 \\ \kappa & 0 & 0 & 1 \end{pmatrix}. \quad (\text{S112})$$

It can be shown that (proof by Laplace expansion and induction)

$$\det [A_M(\kappa) - \lambda I] = [(1 - \lambda)^2 - \kappa^2]^{M/2}, \quad (\text{S113})$$

$$\det A_M(\kappa) = (1 - \kappa^2)^{M/2}, \quad (\text{S114})$$

$$A_M(\kappa)^{-1} = \frac{1}{1 - \kappa^2} A_M(-\kappa), \quad (\text{S115})$$

which suggests that  $\lambda = 1 \pm \kappa$  are the eigenvalues of  $A_M(\kappa)$ , each of which has multiplicity of  $\frac{M}{2}$ . The matrix  $A_M(\kappa)$  is singular when  $\kappa = \pm 1$ .

- 
- [1] Bo Li and David Saad, “Exploring the function space of deep-learning machines,” *Phys. Rev. Lett.* **120**, 248301 (2018).
  - [2] Taro Toyozumi and Haiping Huang, “Structure of attractors in randomly connected networks,” *Phys. Rev. E* **91**, 032802 (2015).
  - [3] Jaehoon Lee, Jascha Sohl-dickstein, Jeffrey Pennington, Roman Novak, Sam Schoenholz, and Yasaman Bahri, “Deep neural networks as gaussian processes,” in *Proceedings of the 6th International Conference on Learning Representations, 2018*.
  - [4] Greg Yang and Hadi Salman, “A fine-grained spectral perspective on neural networks,” arXiv:1907.10599 (2019).
  - [5] Alexander Mozeika, David Saad, and Jack Raymond, “Noisy random boolean formulae: A statistical physics perspective,” *Phys. Rev. E* **82**, 041112 (2010).
  - [6] Petr Savický, “Random boolean formulas representing any boolean function with asymptotically equal probability,” *Discrete Mathematics* **83**, 95 – 103 (1990).
  - [7] Alex Brodsky and Nicholas Pippenger, “The boolean functions computed by random boolean formulas or how to grow the right function,” *Random Structures & Algorithms* **27**, 490–519 (2005).